U.S. DEPARTMENT OF THE INTERIOR

GEOLOGICAL SURVEY

CHROMITE GEOPHYSICS: AN EXAMPLE OF SYNERGISTIC GEOPHYSICAL EXPLORATION FOR INDUSTRIAL COMMODITIES

by

Jeffrey C. Wynn

Open-File Report 81-964

1981

ABSTRACT

Detailed petrophysical studies were made on a suite of rock samples from the Josephine ultramafic complex in northern California in an attempt to see if geophysical methods could be effectively used in the exploration for podiform chromite deposits. In addition, field measurements were made at three chromite deposits by different geophysical methods to determine possible diagnostic contrasts in physical properties of the rock units. Chromite ore appears to normally have low magnetic susceptibility and very high density. Visible and near infra-red measurements of samples indicate that chromite, dunite and harzburgite can be mutally separated by using LANDSAT imagery in relatively unvegetated terranes. Seismic studies indicate that massive chromite gives a substantial velocity increase over the surrounding peridotite, at least in the Sv component, that might be useable in exploration for chromite at moderate depths of burial. Electrical methods show high resistivity and moderate induced polarization effects from massive chromite in field measurements, whereas mono-mineralic chromite in the lab is both electrically inert (virtually no polarization) and highly resistive. Complex resistivity spectra, both in sample and field measurements, show a characteristically jointed or bent shape that appears to be diagnostic of the chromite. This effect might very well be secondary in nature, i.e. caused by cogenetic accessory minerals, and requires additional study in different geologic environments. Throughout these studies, serpentine caused complications, (including strong and irregular susceptibility, density, and polarization variations) that in some cases threatened to obscure any

diagnostic signatures from the chromite; this problem also requires further investigation. These studies imply that integrated geophysical methods could potentially be used on other commodities where geophysical methods have not been used in the past, especially if used in a systematic fashion.

INTRODUCTION

Podiform chromite deposits are found almost exclusively in dunite lenses in a country rock made up almost entirely of harzburgite. The dunite and harzburgite are part of the differentiated mantle material forming the lower unit of the ophiolite stratigraphic sequence (Coleman, 1977). A generalized ophiolite model, showing the approximate location of chromite deposits in this section, taken from Dickey (1975) is shown in Figure 1. An idealized geologic model, showing the somewhat tabular shape typical of podiform chromite bodies, is shown in Figure 2. These bodies are generally composed of 90 percent or more chromite (Mg, Fe'')-$(Cr, Al, Fe'')_2O_4$, usually in the form of grains or nodules packed together. The remaining interstitial material is derived from dunite, and is largely serpentine minerals. The chromite grains or nodules may themselves have an alteration halo, often composed of kammererite, that derives from the serpentinization process (T.P. Thayer, oral communication). The more brittle chromite mass inevitably causes an increased amount of tectonization in its enveloping dunite lens. The consequence, therefore, of the tectonic emplacement process is that the dunite surrounding a chromite pod is usually more heavily serpentinized, presumably because of an increased exposure of fracture surfaces to fluids, than the harzburgite country rock. An argument can also be made, however, that the presence of orthopyroxene crystals makes the harzburgite more resistant to serpentinization. This increased serpentinization implies (though does not necessarily demand) that the magnetic susceptibility increases sharply in the immediate vicinity of a chromite pod, but drops to negligible levels at the chromite mass itself (pure chromite having negligible susceptibility).

Laboratory and field geophysical studies were carried out at three chromite deposits in the Josephine ultramafic complex in collaboration with

studies by John Albers and others during 1978-1979. These studies were an integral part of a U.S. Geological Survey research effort aimed at 1) better understanding the genesis and emplacement of podiform chromite deposits and 2) determining whether an effective exploration strategy for chromite could be developed. Laboratory measurements of a wide variety of physical parameters were made on a suite of 27 rocks from the area, to give direction to follow-up field investigations. Three known deposits were tested by several geophysical field methods. Correlations were then made between the observed geophysical parameters and the mineralogy of the laboratory specimens examined in thin section, and the reported structure and geology of the ore bodies in the field. The rock samples came from the Josephine ultramafic complex with the exception of three which were obtained from nearby chrome-bearing peridotites of the Klamath Mountains. The field sites were chosen with the help of local prospectors, the intent being to geophysically examine known (identified) chromite ore that still remained in the ground, though this has proved to be difficult. The three deposits chosen were the Red Mountain outcrop, Tyson's Mine, and Brown's Mine (Figure 3). Descriptions of the latter two sites are available in Wells, Cater, and Rynearson (1946).

Gravity studies in many different areas (Hammer and others, 1945; Yungul, 1956; Davis and others, 1957; Jancovic, 1963; Bosum, 1963; Parasnis, 1963; Bhattacharyya and others 1969; and Bosum, 1970) indicate that the gravity method is often effective in the search for podiform chromite, but is tedious and expensive, sometimes being unreliable in complex, dissected areas, at least when used by itself.

Magnetic studies have been carried out by several investigators on chromite bodies world-wide (Hawkes, 1951; Yungul, 1956; Bosum, 1963; 1970). These studies indicate that podiform chromite might be more detectable by magnetic methods at greater depths than with gravimetric methods, perhaps sometimes at depths more than twice as great. However, different magnetic susceptibilities and remanent magnetization levels in different regions appear to make this method somewhat site-specific (that is, a geophysical signature, empirically determined from measurements over known deposits, can be used effectively in the local environment where it was determined, but may have only limited usefulness in other localities). In addition, magnetite content in surrounding rocks and in intergrowth contact with chromite nodules will ordinarily vary from area to area. Variations in magnetite content due to variations in amount of serpentinization will also cause extreme fluctuations in the magnetic field over short distances in otherwise "homogeneous" peridotites.

Reid and others, (1980) described ultra-high-frequency seismic reflection experiments used successfully underground in southern Zimbabwe to locate

hidden pods of massive chromite. A single study using induced polarization (IP) in Yugoslavia (Jancovic, 1963) gave equivocal results, mainly because of insufficient IP and geological data. Other geoelectrical studies have come to the author's attention, but these have been unpublished (and usually proprietary) contract survey reports.

LABORATORY STUDIES

Laboratory measurements were made on a suite of 27 rocks collected in and adjacent to the Josephine ultramafic complex of northern California; these studies were made largely to guide the design of subsequent field surveys. This suite is called "original" in Table 1 to distinguish it from additional rocks collected at field geophysical sites later. Three of the samples came from the large Seiad Valley disseminated chromite deposit to the east in the Klamath Mountains. Thin-section analyses were performed on all 27 rocks, and these are adapted by the author for Table 1. The petrophysical measurements made in facilities at the U.S. Geological Survey in Denver, Colo., were described in Hunt and others (1979). Some of the complex resistivity (CR) measurements were made by Zonge engineering, Tucson, Ariz., using facilities described in Zonge (1972). The petrophysical measurements included specific gravity, porosity, grain density, magnetic susceptibility, seismic (compressional) velocity, resistivity and complex resistivity. Radiometric analyses were not made because all the rocks were mafic or ultramafic, and would normally contain very low percentages of radioactive nuclides. Visible and near-infrared reflectance measurements were also made, both of fresh and weathered surfaces; these studies and the instrumentation used are described in Hunt and Wynn (1979). The results of the studies summarized in this section encouraged the application of some of these methods to field experiments described later.

a. Specific gravity

Specific gravity measurements (Figure 4) show a gap in the percentage of chromite that reflects the percentages found in the ultramafic complex; the chromite is either in massive pods or in low-percentage accessory grades distributed through large masses of peridotite. The figure, which combines

Table 1. A summary of the thin section analyses of the original ultramafic complex rock suite
[+Petrography by James Cummings of the U.S. Geological Survey, adapted and summarized by the author.]

SAMPLE	% CHROMITE	%. BLACK OPAQUE MINERALS[1]	% SERPENTINE	% PYROXENE	% OLIVINE	% SECONDARY MINERALS[2]
Brown's Mine	20	75 C	—	—	—	5[d]
279-K-76	—	25 M	75	—	—	--
6-PE-74	90	Minor	—	—	—	Chromite
74-WI-75	Minor	15 M	57	—	—	29[a]
171-K-76	1	9 M	50	8	32	—
21-GA-76	—	10 M	90	—	--	--
40-SE-75	—	8 M	76	15	1	—
SC-4-76	15	—	10	—	75	--
DN-6-76	Minor	12 C	53	26	2	6[b]
278-K-76	Minor	15 M	34	—	5	46[c]
P-6-76	—	10 M	8	89	—	—
69-T-76	—	8 M	92	—	—	--
SC-2-76	—	19 C	2	Minor	80	—
9-PE-74/2	95	—	—	—	—	5[d]
P-7-76	1	10 C	35	—	37	17[e]
45-K-76	—	20 M	80	—	—	—
9-S-76	Minor	4 C?	30	54	11	—
38-S-76	Minor	2 C	18	20	59	--
SC-1-76	12	Minor	2	—	85	—
9-PE-74/1	95	Minor	—	—	—	--
4-PE-74	—	2 C?	13	Minor	69	16[e]
42-S-76	Minor	1 C	41	10	36	11[f]
DN-7-76	Minor	3 C	38	11	48	—
17-WI-75	—	7 M?	58	—	25	5[f]
2-CP-76	1	2 C	9	13	72	3[f]
82-S-76	Minor	4 M	14	5	77	—
Judy Mine	74	14 C	—	—	—	12[d]

1/ Black opaque minerals:

M - Principally Magnetite, determined from magnetic susceptibility

C - Principally chromite, determined from magnetic susceptibility

2/ Secondary minerals:

f. - Actinolite

e. - Iddingsite, calcite, albite

d. - Pargasite, zoesite

c. - Parasitic amphibole

b. - Clinochlor

a. - Serpentine, chromite, sericite, calcite

both percentages of chromite and serpentine, shows nevertheless that massive, podiform chromite is a good target for a gravity survey, at least theoretically. The density contrast between highly serpentinized peridotite and the massive chromite could be as high as 1.6 gm-cm^{-3}, a very large contrast. If the surrounding peridotite is only slightly serpentinized, the contrast may only be 0.8 gm-cm^{-3}, still a significant contrast. Bosum (1963) and Parasnis (1963) have shown that when real-world considerations such as terrain corrections and geologic "noise" (e.g., variations in the amount of serpentinization) are considered, the detectability of a massive pod of chromite may be severely reduced for gravimetric methods. Calculations by Bosum show that the detection limit for a 50,000-ton body under reasonably good circumstances (noise level of 0.2 Mgal and density contrast of 1.4 gm-cm^{-3}) is less than 25 m. Davis and others (1957, 1980) conducted a successful survey in the Camaguey province of Cuba using gravity meters, but the bodies were large, and the topography was gentle. An example of a body from their survey is a 72,000-ton pod, ranging in depth from 23 to 51 m, which contributed an anomaly of 1.4 Mgal.

Further examination of Figure 4 shows a systemmatic behavior of specific gravity with the percentage of serpentine in the rock. As the amount of serpentinization approaches 100 percent, the specific gravity approaches 2.55 gm-cm^{-3}, a result in agreement with Coleman (1971) and Page (1976). Large variations in the amount of serpentinization could cause density contrasts of as much as 0.75 gm-cm^{-3}, a very large source of geologic noise. Davis and others listed 106 anomalies investigated with a drill, of which only 10 were caused by chromite. This survey was economically successful; the point here is that most of the anomalies were caused by the serpentine variation.

Analysis of the porosity of the samples (Figure 5) showed that porosities ranged from 0.176 to 5.06 percent, and had very little correlation with either percent serpentine or percent chromite. Most of the high-serpentine rock samples did have consistently low porosities, which should therefore cause increased resistivity, if the only conduction mechanism is through pore-fluids.

b. Magnetic susceptibility

Figure 6 is a semi-logarithmic combined plot of magnetic susceptibilty versus percent serpentine and percent chromite. Chromite ore shows a consistent pattern of low magnetic susceptibility, at least for samples in the Josephine rock suite, raising the hope that magnetic measurements might be effective in the search for chromite. This behavior is consistent with observations in Greece and elsewhere, but not with results reported by Bosum (1970) for chromite ore bodies in eastern Anatolia. In these examples, Bosum shows that there are magnetic highs consistently associated with the bodies. This, according to Bosum, can be related to the fact that the Turkish chromite deposits, at least in eastern Anatolia, are from the upper part of the (ophiolite stratigraphic) section. The bodies in the Josephine, in Greece, and elsewhere are presumably from a lower part (below the cumulates, in the upper part of the tectonite) of that section. In the Canyon Mountain complex of Central Oregon, Thayer (oral commun.) has observed increased serpentinization and magnetite in immediate contact with the chromite grains, and this may explain the magnetic highs observed there. The magnetite content of a peridotite is controlled to a large extent by the amount of serpentinization, and this problem -- magnetite versus serpentine species -- is currently being investigated.

Bosum (1963) showed that the exploration limit for the magnetic method is substantially greater than for the gravity method: a 50,000-ton orebody might be detectable as deep as 100-200 m with magnetics (0.01 susceptibility contrast, with a 2 nT noise envelope). This should not be regarded as a solution to the chromite exploration problem, however, because again serpentine is a dominant complicating factor. Yungul (1956) considered magnetics less useful in exploring for chromite than gravity due to the high variability of the serpentinization. Bhattacharyya and others (1969) thought that the magnetic results from the Cuttack district of India were unrelated to the chromite, and were determined entirely by serpentinization and other unknown factors. Ghisler and Sharma (1969) suggested that airborne magnetic surveys could be used to find favorable host rocks, but that direct magnetic prospecting for chromite horizons predominantly occurring in anorthosites may not be feasible. A brief examination of Figure 6 does indicate, again perhaps only for the Josephine ultramafic complex, a logarithmic correlation between percent serpentine in the peridotite and the susceptibility of the sample. Remanent magnetization, except in rocks where lightning has induced a strong local component, was generally not significant.

c. Compressional velocity

Compressional velocities in the Josephine suite were studied in the laboratory, and the results may be seen in Figures 7 and 8. There is wide scatter in the velocities (Figure 7) compared with chromite content, undoubtedly due to the serpentine and accessory minerals which are found in varying amounts in the interstices. Samples containing significant olivine, however showed consistently high velocities (Figure 7), more than of 4000 m-sec^{-1}. This may just be the opposite of the results of Figure 8, which show a rough inverse correlation between percent serpentine and velocity; the greater

the serpentine, generally, the lower the compressional velocity. This is readily understandable in terms of the volume of serpentinite traversed by the compressional wave. Typical compressional velocities in pure serpentines are less than 5,600 $m\text{-}sec^{-1}$ whereas in unaltered peridotites the velocities are greater than 7,000 $m\text{-}sec^{-1}$ (Press, 1966). The moderate scatter in the data can probably be related to the presence of orthopyroxene crystals and the complex serpentine morphologies.

d. Visible and near-infrared spectra

Visible and near-infrared spectra of the rock suite (weathered surfaces) show distinct differences between chromite and serpentinized ultramafics, an observation of admittedly little use. There appears to be a usable difference, however, between dunite (the host of 95 percent of the ore found to date) and the ubiquitous harzburgite (Figure 9); this may prove valuable in areas having less vegetation than the Josephine complex. The amount of serpentinization appears to affect the overlying vegetation community strongly. As the amount of serpentinization is also probably related to the tectonic history of an ophiolite slab, it is possible that LANDSAT processing may be useful in narrowing down the size of the potential chromite zones (G. R. Raines and J. C. Wynn, in Prep.). Biogeochemical studies reported by Hawkes and Webb, 1962, and by Brooks, 1972, show that chromite poisons vegetation in a very distinctive manner, and that the amount of serpentinization strongly controls both density and species of vegetation. These studies encourage further field spectrometer and LANDSAT studies in the Josephine complex and other ophiolite environments as well.

e. Electrical measurements

Electrical measurements including resistivity, induced polarization, and complex resistivity spectral shape, were carried out in the laboratory on

samples from the Josephine complex. Initial measurements were carried out by means of a four-electrode system on cored wet samples soaked under a moderate vacuum in doubly distilled water, but resistivities (especially in the massive chromite samples) were so high that the input impedance of the measurement system became a significant contributor to error. A sample of mono-mineralic chromite from Zimbabwe measured dry with a two-electrode system (described in Hunt and others, 1979) gave resistivities at 10 Hz. of more than a megohm-meter (Olhoeft, written commun., 1977). The samples were therefore dried, and resoaked in a 100 ohm-meter solution of KCl (0.72 mg KCl per liter).

Figure 10 shows comparisons of resistivities versus percent chromite and percent serpentine. In Figures 10 and 11, the lines connecting the data points represent repeated measurements of the same sample. The moderate variation observed should not be disturbing, implying only that the samples were not completely in equilibrium with the pore fluid at the beginning of the measurement process. The variations were not in any consistent direction with time.

In these studies, massive chromite samples had resistivities that ranged from less than 1000 ohm-meters to more than 20,000 ohm meters. There appears to be no correlation between percent chromite and resistivity, at least for the samples in this suite from the Josephine complex (the following section does, however, show resistive highs associated with chromite outcrops in field measurements). Serpentine showed only the very weakest correlation, with a slight preference for lower resistivity for higher percentages of serpentine. This poor correlation is surprising; common understanding among geophysicists (see, for instance, Fig. 1 of Keller and Frischknecht, 1966) is that serpentine has a relatively low resistivity. The lack of correlation between resistivity and chromite, and poor correlation between resistivity and

serpentine indicates that other factors are therefore strongly involved in the conduction of current in the Josephine rocks. Figure 11 shows a comparison between resistivity and porosity, but despite the low resistivity of the pore-fluid, there is only a weak correlation with the porosity in the measurements. In the megascopic scale, of course, fracturing will have a stronger influence on the resistivities than seen in these laboratory measurements, where samples were carefully selected and cored to be fracture free. Several factors may cause the scatter seen in these two figures, among them the diverse mineral content. The serpentine morphology (in other words, the number and orientation of the serpentine veinlets) may affect scatter and the serpentine species may also be involved. There is some evidence (Page, oral commun.) that clinocrysotile may be preferentially conductive along the axis of the fibers, whereas lizardite and antigorite may not be nearly so anisotropic, or even as conductive. Studies by Zablocki (1964), and Stesky and Brace (1973) indicate that a significant conduction mechanism in some serpentinites may be magnetite along clinocrysotile veinlets, a byproduct of the serpentinization process. The irregularity of the apparent mineral conduction component may be tied to the tectonic history of the rock, perhaps through a gradient in oxygen fugacity. Studies are currently underway to try to resolve these questions.

Induced polarization measurements (Sumner, 1976) were made on the rock suite and showed a similar wide variation in behavior (Figures 12 and 13). This variation or scatter held for both the chromite and serpentine percentages (no relationship at all was observed for the other minerals present). The values shown in these figures are the phase-angle shift (in milliradians) between the input and the output current waveforms at the 0.1 hz fundamental frequency.

Common belief among geophysicists also has it that serpentine is a highly polarizable material, but this also is not necessarily true for the rock samples of the Josephine suite (see Figure 13). Almost certainly the polarizability of serpentine-rich rocks depends on morphology and the species of serpentine. Chromite samples had a moderate polarizability apparently unrelated to the chromite percentage. Samples containing black opaque minerals, however, and having high magnetic susceptibilities have unusually high polarizability (solid triangles in Figure 12). Magnetite by itself is not known to cause such a degree of polarization (Zonge and Wynn, 1975, p. 858). As serpentine often strongly saturates complex resistivity spectra, (see following paragraphs) there may be a relationship between magnetic susceptibility and a particular serpentine species that might be used to permit deeper electrical detection. (If a readily characterizable relationship between serpentine species and content, and electrical behavior, can be found, it could theoretically be removed). This problem is currently being studied by means of petrographic and X-ray analysis to separate the serpentine species.

Electrical spectra or complex resistivity studies were made on the original suite of 27 samples from the Josephine, as well as on rocks collected from the sites where the field work (described later) was carried out. Figure 14* shows five spectra from the Josephine suite, separated and arranged in order of pyroxene content. This was done in an attempt to distinguish dunite from harzburgite. Virtually all podiform chromite masses are found in close

* Figure 14 and subsequent spectral plots in this paper are Argand Diagrams, with results plotted in the Cartesian Complex Plane, negative imaginary direction being "up", with all values normalized to the lowest frequency real component; the frequencies increase logarithmically from the right.

association with dunite (usually enclosed in a lens of it); the dunite itself is found sporadically in the more ubiquitous harzburgite, which in turn is by far the major constituent of the tectonic peridotite. The rather arbitrary convention that separates harzburgite from dunite is that the latter is peridotite containing less than 10 percent orthopyroxene, whereas the former is peridotite containing more than 10 percent orthopyroxene.

The three dunite spectra in Figure 14 (P-7-76, SC-4-76, SC-2-76) are clearly different from the two harzburgite spectra (38-S-76 and 171-K-76). An attempt to correlate the spectra with mineral content (see Table 1) shows that only a rough dunite/non-dunite characterization can be made on the suite; the percent of serpentine, for instance, does not correlate very well with the spectral shapes. An attempt was made to try to characterize the spectra in a quantitative fashion by fitting them to Cole-Cole dispersion equations (Walter Anderson, unpub. program) as suggested by Pelton and others (1978). The results of the curve-fitting are included in the plots in Figure 14; a solid line indicates the original data, and the triangles indicate the best Cole-Cole fit obtained. A discussion of the Cole-Cole equations used is found in the Appendix to this paper, along with a tabulation of the derived parameters (Table 2). A comparison of the derived parameters with the dunite/harzburgite contrast shows a weak correlation with only one of them: The Ro or amplitude-change parameter. The Ro parameter is strongly influenced by the amount of serpentinization, however, and this (instead of the orthopyroxene) is probably the reason for the correlation. Although the curves can generally be made to fit most smoothly varying spectral shapes, the actual resolution of the parameters (shown by the $\pm$ terms in the Appendix) is quite often very poor. Zonge (1972) suggested another curve-fit approach based on an electrical circuit analog. This model was fitted to 10 of the Josephine spectra, but

efforts to correlate parameters of this model with ultramafic petrography were even less successful. Zonge and Wynn (1975) suggested another, empirical approach at spectral categorization based on the rate of change of the imaginary component of the spectra as a function of the frequency. This classification scheme was originally derived from studies of altered porphyry systems, and is not particularly designed for the rock spectra from the Josephine suite. It remains an alternative, however, that will be shown to be at least partly successful later on. These letter classifications are discussed in the Appendix, and all spectra included in this paper are classified in Table 2 along with Cole-Cole and Zonge parameters obtained.

During the course of the field work (described in the next section) several representative hand-samples were gathered from the mineralized field sites. Although detailed thin-section data are unavailable, several samples that were clearly massive chromite were measured for electrical spectral shapes, and the results were combined with massive chromite samples from the Josephine suite to give the spectra in Figure 15. With one exception, these spectra show that chromite ore gives lower imaginary values at higher frequencies than at lower or intermediate frequencies. The spectra also have a total real component variation from lowest to highest frequencies of 0.08 - 0.28 (in other words, weakly to moderately polarizable) when normalized by the lowest frequency real component. In the spectra so far observed from the Josephine ultramafic complex, this translates to a "bent" or jointed spectral shape (in other words, an increase followed by a decrease of the imaginary component as frequency increases).

When the Cole-Cole fits were done on these spectra, it was noted that this spectral flexure corresponded to a relaxation time τ that ranged from 0.2 to 3.5 for three of the samples, and that was 140 for the fourth (6-PE-74).

This translates to a broad imaginary component peak centered between 0.3 and 60 Hz (0.007 Hz for 6-PE-74). No other parameters of the Cole-Cole family of equations correlated with the presence of massive chromite in the samples. The exceptional spectrum of BLD-BRM is more nearly characteristic of an inert rock (i.e. electrically non-responsive) than it is of a chromite-rich rock, but complete thin-section information on it is unavailable. Most of the peridotite measured had spectral shapes like those of Figure 16, both of which have relaxation times smaller than about 10^{-4}. These two spectra are for peridotite samples collected at the Red Mountain field site described later), and although thin-section data are unavailable, both contained more than 40-50 percent serpentine in hand-sample examination. The limited experience obtained so far indicates that these spectra may be characteristic of serpentinized peridotite that contains little or no chromite.

f. Summary of laboratory studies

All of the laboratory electrical studies carried out suggested that chromite, at least in massive form, could be separated from the surrounding peridotite. This led to the field experiments described in the next section, and as will be seen, accurately predicted the results obtained there. Several caveats go with this information, and they should be discussed here. First, an unusually large number of variables are involved, including mineral content, rock texture (in the microscopic sense), and the measurement and preparation history of the samples. Strong evidence also suggests that different serpentine species respond differently to electrical measurements (preliminary indications, for instance, point to the highly reactive nature of clinochrysotile in polarization measurements relative to lizardite and antigorite). As of this writing, the serpentine species of the samples described have not been successfully sorted out. The effects of serpentine

generally in the electrical spectra apparently are nevertheless substantial, and may make it difficult to sort out the spectral behavior of the chromite from that of highly serpentinized peridotite. In view of the very high resistivity and unusually low solubility of the pure chromite mineral (implying potentially small double-layer and ionic phenomena), the electrical spectral characteristic observed is probably due to mineral or morphological phenomena fortuitously associated with the chromite, and not due to the chromite directly. This raises the possibility that the apparently diagnostic electrical spectral shape may be site-specific (i.e., unique to only one local area), as we already know the magnetic susceptibility often is. A new variable, megascopic texture, is introduced in the next section where field measurements are described.

FIELD STUDIES

Ground magnetic, electromagnetic (EM, both VLF and Slingram), and complex resistivity (CR) studies, as well as limited seismic-refraction studies, were made at several locations in the Josephine complex. CR measurements were made at the three principal sites: Brown's, Tyson's and the Red Mountain outcrop deposits. The Tyson's Mine CR results (obtained with an experimental U.S. Geological Survey system) were unusable, because of instrumentation problems, and are therefore not included in this paper. The seismic data are only partly recoverable because of an intermittent noise problem with the recorder system, but data from Red Mountain was successfully processed, and will be shown. The following discussion will cover the Red Mountain outcrop, Tyson's Mine and Brown's Mine in that order.

A. Red Mountain outcrop

The Red Mountain site consists of two small chromite outcrops below the crest of a steep hill near the southern tip of the Josephine ultramafic sheet (Figure 1). Some dunite is found in contact with the chromite but very little is visible elsewhere at the site, where the ground (except for the chromite outcrops) is covered with harzburgite scree. The outcrops consist of massive brecciated ore, (including fragments of serpentinite and mineralized blocks that might locally be 90 percent chromite) partly fractured and rehealed, in contact with strongly tectonized dunite. The surrounding peridotite is estimated to be about 50 percent serpentinized.

The VLF-EM apparent-resistivity profile (Figure 17C) shows resistive highs over both outcrops; cross lines and one parallel line (not shown here) indicate that these resistive highs are localized around the outcrops. This may be caused solely by the absence of soil on the outcrops; however, the total field magnetic data (Figure 17B) show a high at the western edge of the

western outcrop, with a sharp 550 nT (Nanotesla, where 1 nT=1 gamma) magnetic low over the central and eastern part of the outcrop. It can be argued that this magnetic low extends eastward through the other (easternmost) outcrop, and then gives way to a high, followed by another low that is unexplainable from the surface geology. The magnetic low may be caused by a remanent magnetization effect, but is most likely due to the absence of the more magnetic peridotite, the space being occupied instead by the low susceptibility chromite mass. The sharp magnetic high at the western edge of the west outcrop is probably caused by the increased serpentinization of the dunite halo. The extensive tectonization and serpentinization of the ophiolite mass diminish the importance of the remanent portion of the magnetization. In only one case was remanence a significant contributor, and that was due to an apparent lightning strike on an exposed outcrop of harzburgite.

Figure 18 shows apparent resistivity and phase-angle pseudosections. These are conventional induced polarization (IP) data, a byproduct of the CR survey. The apparent resistivity data show resistive highs associated with both outcrops, (subtle in the case of the eastern one) in agreement with the VLF-EM results of the previous figure. The phase-angle data indicate that the outcrops are somewhat more polarizable (2 to 5 milliradians in a half-milliradian-precision survey) than the surrounding peridotite. These data also indicate that the eastern outcrop has a finite depth extent, perhaps less than 5 m, but that the western outcrop (or at least the source of the polarization) extends below the range of the survey method. For a 10-m dipole spacing, (distance between electrodes of the receiver) this implies a depth of at least 20 m in this kind of electrically resistive terrane; a larger dipole spacing would "see" deeper but would also provide less resolution.

Figure 19B shows a pseudosection of spectral shape response interpreted from CR measurements taken along the traverse. These are the spectral characterizations of Zonge and Wynn (1975) described in the previous section and in the Appendix. Figure 19C shows two representative field CR spectra. At Red Mountain, only two spectral shapes were observed, the "C" and the "Cc". In the latter spectrum, the lower frequency part of the spectral curve increased steeply but leveled off after 1.0 Hz: therefore the double character representation for a "bent" spectrum. Recalling the discussion about laboratory chromite samples, we were looking for a "peaked" or "bent" CR spectrum. The "Cc" spectral shape observed beneath the two outcrops is almost certainly related to the same spectral shape observed in the laboratory for chromite samples. The high-frequency end has not decreased as much as in the the imaginary component, because the field results are a weighted average of the results for chromite and a much larger volume of peridotite surrounding the chromite. A Cole-Cole fit was done on the "Cc" spectrum, but because of the "dilution" effect of the surrounding peridotite, a (possible) relaxation time in the 0.2-3.5 range could not be resolved. The bend does, however, occur at about 1.0 Hz, leaving the letter characterization as the only effective way of separating the two different spectral types. The spectral-type pseudosection again shows the outcrop on the east to have limited extent, but the apparent chromite signature shows that the outcrop on the west side goes to depth. This apparent extension to depth is the same result as that obtained with the phase-angle data, but it appears much more diagnostic.

Figures 20 and 21 show the results of two shear-wave refraction profiles (Wynn and Hasbrouck, 1980) using a 12-channel portable seismic system over the western outcrop at the Red Mountain (California) site described previously. The data in Figure 20 represent a two-layer earth with a sharp variation in

the second segment of the travel-time curve over the outcrop. This bulge in the curve is caused by a substantial velocity increase in the chromite. Figure 21 is nearly identical with Figure 20, except that the shotpoint is moved to the other side of the outcrop and geophone array to check against the possibility of some purely geometrical effect.

The magnitude of the velocity increase (perhaps a factor of two or more) is such that a similar podiform chromite deposit might be readily identifiable at substantial depth, depending on its size and the presence of other inhomogeneities. The magnitude of the velocity anomaly may be enhanced by the amount of serpentinization in the surrounding rock; consequently an unserpentinized host peridotite might not provide quite so large a velocity contrast. Along with the reflection studies of Reid and others (1980), this work suggests that seismic methods may be the best single exploration approach for podiform chromite discovered so far.

The full results of seismic measurements at the Red Mountain site, and results at the other two mines and a fourth experimental location, are part of an ongoing study. It appears, however, that the chromite deposits at Red Mountain give resistivity, magnetic, IP phase angle, CR spectral shape, and shear-wave (Sv component) velocity anomalies. All the geophysical data are consistent with (but not necessarily indicative of) a dunite lens stretching from the west outcrop to the east outcrop, including in it a massive chromite outcrop on the west which extends to a depth of at least several tens of meters. The single "Cc" spectrum observed beneath stations 5-6 is also consistent with this model, and may imply a small amount of chromite in the middle of the dunite lens.

B. Tyson's Mine

Tyson's Mine is located 5 km south of Gasquet, Calif., in the south-central part of the Josephine ultramafic sheet on a steep slope where it has been exposed by mining (Figure 1). Most of the original chromite ore has been mined out, but Mr. Bill Whippo, the last mine foreman to work there, described a pod of chromite that had been found by a drift just as the mine was shut down. The pod is in a white, heavily serpentinized and sheared peridotite which in turn lies beneath weathered, weakly metamorphosed greenstone. The greenstone unit apparently is in fault contact with the underlying serpentinite, and probably represents the pillow-lava part of the ophiolite stratigraphic section.

Figure 22 shows the topography, the geologic relationships, and the reported location of the chromite pod. The total field magnetic profile shows a 500 nT low (this could be at least partly a contact effort) over the chromite pod, whose diameter and shape are not well defined; a 10 m horizontal dimension, however, was estimated by Whippo. There is a broad VLF-EM resistivity low over the exposed areas of white serpentine, but apparently no influence or effect from the chromite pod can be clearly discerned in this data. The VLF-EM apparent resistivity profile is also interesting in that the resistivities are unusually low in comparison with the other sites visited, over the entire length of the traverse. The entire surface has been exposed by hydraulic mining, and the serpentinization is extensive, often reaching 100 percent in hand-sample examination.

C. Brown's Mine

Brown's Mine is on the southern flank of Low Plateau, about 10 km north of Gasquet, Calif., and 5 km south of the Oregon border. It is in a harzburgite terrane that is cut by sparse 10-50 m-wide layers of dunite that

generally strike north, and numerous but small (5-30 cm wide) variable-length layers of dunite. In the mine area, there is a gentle 15 to 20 degree eastward dip in the foliation of the harzburgite. The serpentinization is on the order of 25-45 percent, in some places going to nearly 100 percent. The chromite itself was exposed by erosion on the north side of a steep ravine. It is massive, typically 75 - 95 percent chromite, containing 5 - 25 percent interstitial material made up largely of pargasite (?), zoesite, chlorite, and olivine. The podiform bodies have yielded around 20,000 tons of chromite and an estimated 5,000 tons at least remain in the ground but are currently inaccessible.

Figure 23 shows a topographic profile, and the apparent resistivity and phase-angle pseudosections. The data were obtained on a line about 40-45 m above the known extensions of the remaining ore (centered below station 4); the location was obtained from old mine maps and from on-site observations. The apparent resistivity pseudosection shows resistivities ranging from about 300 to 2,500 ohm meters. These values are much higher than those obtained at Tyson's Mine, and even higher than the resistivities at the Red Mountain outcrop, but not unreasonable for a moderately serpentinized peridotite. The diagonals on the east end in figure 23B show that lower resistivity values are caused by areas of highly serpentinized peridotite exposed at the surface and apparently extending to depth.

Figure 23C shows the phase-angle pseudosection, where the same diagonals that show lower resistivities in Figure 22B now indicate higher polarizability--this is the serpentinite showing up again. To an experienced interpreter familiar with the gentle eastward dip of the foliation, the subtle but consistent 35 degree westward dip in the pseudosection contours would indicate a westward dip in the serpentinite mass outcropping around stations 7

to 10. Geologic information at the surface and in the pit area of the massive chromite body indicate no abrupt structural changes in the area, which means that the somewhat more shallowly westward dipping contours must be caused by some discrete polarizing feature nearly masked out by the strong serpentinite effect. This feature coincides with and extends slightly east of the known remaining chromite ore. A possible eastern extension of the ore zone downdip was suspected by the operators at the time the mine was shut down, but uncertainties in line location, the amount of serpentinization, and the imperfect two-dimensionality of the deposit make the chromite extension difficult to pin down more exactly, either geophysically or geologically.

Figure 24 shows representative Argand diagrams of CR spectra observed in field data from Brown's Mine. These spectra are labeled according to the convention described in the Appendix. Three examples of a fifth spectral type (tentatively labeled "Ac" by the prevously described convention) were obtained but were only type "A" spectra, with high-frequency imaginary-component artifacts caused by electromagnetic coupling, (Wynn and Zonge, 1975; Pelton and others, 1978) and are not represented here. The spectral shape of most interest is the "Cb" curve on the top of the figure. Using the Cole-Cole fit, a relaxation constant of 0.029 was obtained for this spectrum, but without the serpentine "dilution" would probably have been closer to 1.0 because the largest imaginary component is at 1.0 Hz. If the laboratory and Red Mountain field observations are applicable to Brown's Mine, the places where this shape is found in the pseudosection should correspond to the chromite ore.

Figure 25 shows the interpreted spectral shape pseudosection for Brown's Mine. The "C" and the "A" contributions appear to be caused by an increase in serpentinization; why two different contributions exist is not yet clearly understood; more complete subsurface geologic information along the line might

supply an explanation. In the center of the pseudosection, a discrete block of material having the "Cb" spectral characteristic is located at and extends slightly west of the known location of the chromite ore. There is another discrete zone on the eastern edge of the pseudosection, just beyond the serpentinized area, but there is also insufficient geologic information to allow any identification of this eastern anomaly. These results (excluding this unknown eastern zone) seem to bear out the laboratory observations that a spectrum with increasing, then decreasing, imaginary component as a function of frequency (a jointed or flexed spectrum in an Argand diagram) is indicative of the presence of massive chromite. The casual relationship between chromite and flexed spectrum is not understood at this time, and we should anticipate the possibility that the association is indirect, and therefore at least potentially site-specific. Laboratory studies are underway to attempt to answer the question about the nature of the relationship between massive chromite ore and the apparent chromite CR signature.

For the sake of completeness, the total field magnetic profile has been included in Figure 25. Perhaps the most important piece of information contained in the traverse is a caveat: in a serpentinized terrane, the magnetic field can be expected to vary wildly. The high amplitude, short wavelength anomaly over the mineralized zone has a spatial variation (3,000 nT in only 15 m horizontal distance, measured 3-m above the surface) so short that the source must be virtually at the surface. Careful examination of the rocks showed no significant variation in rock type, percent serpentine, or structure. When a low-pass spatial filter was applied to the data (Figure 26), a magnetic low did remain over the ore zone and extended to the east as does the polarization anomaly. On the eastern side of the line a broad magnetic high was observed, which correlates with an area of nearly 100

percent serpentinized rock on the surface; a profile completed 20 m to the north of the serpentinite did not give a similar anomaly.

The geophysical data at Brown's Mine gave very encouraging results; the CR spectra, the magnetic data, and to a lesser extent the phase-angle data, all have correlatable anomalies. In all cases, however, the degree of serpentinization influenced the data and obscured its interpretation, in places to the point where if a massive pod of chromite existed, it might not be uniquely identifiable if only a single method tied to only one physical property were used.

CONCLUSIONS

In this paper it has been shown that gravity, magnetic, seismic, and electrical methods might all be used with varying degrees of success in the exploration for podiform chromite, at least in the Josephine ultramafic complex. These results, however, have broader implications, and three general observations, all interrelated, can be made from them. The first is that some of the geophysical anomalies correlatable with chromite deposits are secondary or associative in nature. The geophysical signature may be indicative of another, associated accessory mineral or physical property, and not the chromite. This might explain why one of the chromite lab samples failed to give a jointed or flexed spectral signature, for instance (there are other, more mundane reasons, like poor sample handling techniques, etc.). A magnetic high would certainly be associative, but a magnetic low could be a direct indicator. If a particular geophysical signature is associative, it runs the risk of being site-specific; in other words, it might work in the Josephine peridotites but not in other peridotite areas of the nearby Klamath Mountains. For this reason the research is now moving in two directions: a) check the geophysical signatures at other locations, and b) sort out the nature of the mineralogic/geophysical associations with detailed x-ray and petrographic work using control samples.

The second general observation is that any one geological or geophysical signature in and by itself is usually insufficient justification for a drill hole. There might be hundreds of magnetic lows, and perhaps hundreds of small gravity highs, in a given target area. There would, however, be a fewer number of localities where the gravity highs and magnetic lows coincide. If a seismic-velocity high or a flexed CR spectrum was observed over several anomalies, a project geophysicist could recommend a drillhole.

This second observation, that several coincident physical-property signatures offer the best chance for a unique identification of a chromite pod, leads naturally to the third observation. Seismics and Complex Resistivity are the most diagnostic methods discovered so far in the research in northwestern California. These methods are also, by far, the most expensive. A seismic survey of the 20 by 60 km Josephine ultramafic sheet would be prohibitive from an economic point of view; the cost of the survey would exceed that of the economically realizable reserves, (see, for example, the calculations in Menzie and Singer, 1980) and it would take years to complete. The logical alternative, of course, is to initiate a systematic exploration program where the method that is least costly per square kilometer is used first, followed by other methods in a sequence based partly in order of expense and difficulty, working on smaller and smaller parcels of land that are thought to have the highest potential based on earlier, less diagnostic surveys. The first two surveys, perhaps LANDSAT and aeromagnetic, would both have to cover the entire tract of land, unless geologic information permitted a start on a smaller parcel initially - for instance by excluding the keratophere, sheeted dike, and pillow-lava complexes. Geochemical surveys would probably not be useful because of the very low solubility of chromite and ubiquitous presence of accessory grade chromite throughout the peridotite.

Finally this study suggests that geophysical methods could potentially be used on many other commodities where geophysics has not been widely used in the past, for instance potash, titanium, or tungsten. The main requirement is that a careful sampling survey, followed by detailed laboratory studies, be made in a given area of high potential. The degree of success in exploration

for these types of commodities may largely depend on the degree of cooperation between geophysicists and geologists, and the utilization of the largest possible range of tools in a systemmatic manner.

ACKNOWLEDGEMENTS

James Cummings did the thin-section analyses of the original Josephine rock suite, and Steve Manydeeds and Karen Christopherson did much of the laboratory petrophysical studies. Bruce Smith and Gary Olhoeft offered invaluable advice and access to facilities for the laboratory electrical measurements. The largest part of the complex resistivity field measurements and most of the attendant data-processing were done by Zonge Engineering and Research, and the seismic measurements were made by Bill Hasbrouck and the author. Charles Henry did many of the plots for the electrical data, and Tom Hildenbrand filtered the Brown Mine magnetic profile. Lee Hescock of Crescent City, California, and Mr. and Mrs. Eugene Elliott of O'Brien, Oregon gave permission to work on their properties, as well as access to all mining records. This study owes much to John Albers, who suggested the study and lent geologic advice and encouragement with unflagging enthusiasm.

REFERENCES CITED

Bhattacharyya, B. B., Mallick, K., and Roy, A., 1969, Gravity prospecting for chromite at Sukinda and Sukrangi, Cuttack district, Orissa (India): Geoexploration, v. 7, p. 201-240.

Bosum, W., 1963, Theoretical limits of the application of geophysical methods: Organization of Economic Cooperation and Development (O.E.C.D.) Symposium on methods of prospection for chromite, Athens, Greece, 1963, p. 209-224.

Bosum, W., 1970, An example of chromite prospection by magnetics: Geophysical Prospecting, v. 18, p. 637-653.

Brooks, R. R., 1972, Geobotany and biogeochemistry in mineral exploration: New York, Harper and Row, 290 pp.

Cole, K. S., and Cole, R. H., 1941, Dispersion and absorption in dielectrics: Journal of Chemical Physics, v. 9, p. 341.

Coleman, R. G., 1971, Petrologic and geophysical nature of serpentines: Geol. Soc. American Bull., v. 82, p. 897-918.

_____1977, Ophiolites: New York, Springer-Verlag, 229 p.

Davis, W. E., Jackson, W. H., and Richter, D. H., 1957, Gravity prospecting for chromite deposits in Camagüey province, Cuba: Geophysics, v. 22, p. 848-869.

Davis, W. E., Jackson, W. H., and Richter, D. H., 1980, Exploration for Chromite in the Camaguey District, Camagüey Province, Cuba: U.S. Geol. Survey Open-File Report 80-1061.

Dickey, J. S., Jr., 1975, A hypothesis of origin for podiform chromite deposits: Geochimica et Cosmochimica Acta, v. 39, p. 1061-1074.

Ghisler, M., and Sharma, P. V., 1969, On the applicability of magnetic prospecting for chromite in the Fiskenaesset region, west Greenland: Gronlands Geologiske Undersogelse Rapport, no. 20, Geological Survey of Greenland.

Hammer, S., Nettleton, L. L., and Hastings, W. K., 1945, Gravimeter prospecting for chromite in Cuba: Geophysics, v. 10, p. 34-49.

Hawkes, H. E., 1951, Magnetic exploration for chromite: U.S. Geol. Survey Bull. 973-A, p. 1-21.

Hawkes, H. E., and Webb, J. S., 1962, Geochemistry in mineral exploration: New York, Harper and Row.

Hunt, G. R., and Wynn, J. C. 1979, Visible and near-infrared studies of rocks from chromite-rich areas: Geophysics, v. 44, no. 4, p. 820-825.

Hunt, G. R., Johnson, G. R., Olhoeft, G. R., Watson, K., and Watson, D. E., 1979, Initial report of the petrophysics laboratory: U.S. Geological Survey Circular 789, 74pp.

Jancovic, A. S., 1963, Prospecting for chromite deposits in Yugoslavia: Organization of Economic Cooperation and Development (O.E.C.D.) Symposium on methods of prospection for chromite, Athens, Greece, 1963, p. 203-208.

Keller, G. V., and Frischknecht, F. C., 1966, Electrical methods in geophysical prospecting: New York, Pergammon Press, 517 p.

Menzie, W. D., and Singer, D. A., 1980, Some quantitative properties of mineral deposits, in Meyer, R. F., and Carman, J. S., eds., The future of small-scale mining: New York, McGraw-Hill.

Page, N. J., 1976, Serpentinization and alteration in an olivine cumulate from the Stillwater complex, southwestern Montana: Contrib. Mineralogy and Petrology, v. 54, p. 127-137.

Parasnis, D. S., 1963, Some aspects of geophysical prospecting for chromite: Organization of Economic Cooperation and Development (O.E.C.D.) Symposium, p. 225-231.

Pelton, W. H., Ward, S. H., Hallof, P. G., Sill, W. R., and Nelson, P. H., 1978, Mineral discrimination and removal of inductive coupling with multifrequency IP: Geophysics, v. 43, no. 3, p. 588-609.

Press, F., 1966, Seismic velocities, in Clark, S. P., ed., Handbook of physical constants: Geological Society of America Memoir 97, p. 198-200.

Reid, A. B., Polome, L.G.B.T., and Green, B. W., 1980, Ultra-high resolution reflection seismology in chromite detection: Geophysics, v. 45, no. 4, p. 578.

Seigal, H. O., 1959, Mathematical formulation and type curves for induced polarization: Geophysics, v. 24, no. 5, p. 547-565.

Stesky, R. M., and Brace, W. F., 1973, Electrical Conductivity of serpentinized rocks to 6 kilobars: Journal of Geophysical Researcn, v. 78, no. 32, p. 7614-7621.

Sumner, J. S., 1976, Principles of induced polarization for geophysical exploration: New York, Elsevier, 277pp.

VanVoorhis, G. D., Nelson, P. H., and Drake, T. L., 1973, Complex resistivity spectra of porphyry copper mineralization: Geophysics, v. 38, no. 1, p. 49-60.

Wells, F. G., Cater, F. W., Jr., and Rynearson, G. A., 1946, Geologic investigations of chromite in California, Part I - Klamath Mountains: California Dept. of Natural Resources and Division of Mines Bull. 134. 76 p.

Wynn, J. C., and Hasbrouck, W. P., 1980, Geophysical studies of chromite deposits in the Josephine ultramafic complex of northwest California and southwest Oregon: U.S. Geological Survey Open-File Report 80-936, 16 p.

Wynn, J. C., and Zonge, K. L., 1975, EM coupling, its intrinsic value, its removal, and the cultural coupling problem: Geophysics, v. 40, no. 5, p. 831-850.

Yungul, S., 1956, Prospecting for chromite with gravimeter and magnetometer over rugged topography in east Turkey: Geophysics, v. 21, no. 4, p. 433-454.

Zablocki, C. J., 1964, Electrical properties of serpentinite from Mayaguez, Puerto Rico: in A study of Serpentinite, N.A.S.-N.R.C. Publication 1188, p. 107-117.

Zonge, K. L., 1972, Electrical properties of rocks as applied to geophysical prospecting: Tucson, Univ. of Arizona PhD dissertation, 156 p.

Zonge, K. L., Sauck, W. A., and Sumner, J. S., 1972, Comparison of time, frequency and phase measurements in induced polarization: Geophysical Prospecting, v. 20, p. 626-648.

Zonge, K. L., and Wynn, J. C., 1975, Recent advances and applications in complex resistivity measurements: Geophysics, v. 40, no. 5, p. 851-864.

APPENDIX

The introduction of the Complex Resistivity method (Zonge, 1972; VanVoorhis and others, 1973) gave an added dimension of information to explorationists and earth scientists, making available spectral plots of received amplitude and phase as a function of frequency. This new source of information does present one major problem: how to describe the spectral shapes that are obtained. There are two major approaches: fit analytical curves to the spectra by a least-squares method, or arrive at an empirical description. Both methods have advantages and disadvantages. Zonge (1972) and Pelton and others (1978) took the former approach, made certain assumptions about the nature of the electrochemical interaction responsible for the transfer functions, derived or adapted analytical equations for those interactions, and then fitted curves using those equations to the data. The parameters or variables of the best fit then presumably describe the process that has taken place in the rock or earth that was being sampled. The disadvantages of this approach are that the initial assumptions may not hold, and some spectra, such as the apparently diagnostic "bent" or jointed chromite spectra, are not readily described by any of the parameters of the above-mentioned approaches. An alternative, empirical descriptive approach was originally described by Zonge and Wynn (1975). The disadvantage of this empirical curve-shape typing method is that it is even less related to any real-world physical or electrochemical phenomena. Both approaches, incidentally, are susceptible to non-unique interpretations.

Zonge (1972) devised a method based on the use of five parameters, listed and described below, utilizing the following equation:

$$Z = \frac{R_{dc}}{(AN+1)\theta} \left\{ AN \cdot \theta + \tanh(\theta) \right\} \qquad (1)$$

...where $AN = \frac{R_{ac}}{R_{dc}-R_{ac}}$ and

$$\theta = \sqrt{\frac{(AN+1)R_{dc}}{2} \left[\frac{A_k C_{dl} R_{ct} (i\omega)^{3/2} + C_{dl} (i\omega) + A_k (i\omega)^{1/2}}{A_k R_{ct} (i\omega)^{1/2} + 1} \right]} \qquad (2)$$

This is the complex impedance of the rock. In these equations,

C_{dl} is the double-layer capacitance

R_{ct} is the charge-transfer resistance

A_k is the Warburg admittance

R_{dc} is the resistivity in the zero-frequency limit

AN is a measure of blocked vs. unblocked pore spaces, and is roughly related to chargeability.

Ten of the spectra included in this paper were fitted to this equation, and are tabulated for completeness' sake in Table 2. The details of the derivation of the equation are in Zonge (1972), along with the distributed circuit used as the rock analog.

Pelton and others (1978) took an alternative approach, and used equations derived originally by Cole and Cole (1941) for electrode-electrolyte interactions. In the form used by Pelton these equations have either four or seven parameters, used to fit single or double dispersion phenomena respectively. These equations and their parameters are as follows:

$$Z = R_o \left[1 - M \left(1 - \frac{1}{1 + (i\omega\tau)^C} \right) \right] \qquad (3)$$

...The single-dispersion equation, and

$$Z - R_o \left[1 - M_1 \left(1 - \frac{1}{1+(i\omega\tau_1)^{C_1}}\right)\right] \cdot \left[1 - M_2 \left(1 - \frac{1}{1+(i\omega\tau_2)^{C_2}}\right)\right] \quad (4)$$

... for a fully - resolvable second dispersion. This latter is the seven-parameter equation, and was the only one used to fit several of the curves represented in this paper. All other curves were fitted using equation 3. In these equations,

R_o is the lowest frequency resistivity of the sample (in these cases, normalized to one)

M is the chargeability described by Seigel (1959)

τ is the relaxation time constant

C is the frequency dependance of the phase (slope)

...and the subscripts indicate which dispersion the parameter describes. The parameters of all curves represented in this paper, derived from the single- or double-dispersion Cole-Cole curve fit are given in Table 2.

A third method of characterization of complex resistivity spectra is an empirical letter designation along the lines first suggested by Zonge and Wynn (1975). In this classification scheme, spectral curves are characterized, segment by segment, by a letter describing their slope on an Argand diagram. A curve that has a sharp decrease of imaginary component as frequency increases (also as real component decreases) is called "A" - type. If the slope is very shallow, but still decreasing, the curve is labeled "a". Curves with a flat (e.g. constant imaginary component) slope are labeled "b". Spectra that have a steeply increasing imaginary component (increases upwards to the left) as frequency increases are labeled "C", whereas a shallow increasing curve is given the label "c". When spectra bend or pitch up, or otherwise show evidence of a clear dispersion or an electromagnetic coupling component, then the curve can be described segment by segment, beginning at

the lowest frequency end. A curve therefore that has the apparently diagnostic "chromite bend" could be described in simplest form as "Ca", or if the dispersion is diluted by another dispersion with a relaxation time constant τ fairly close to the first (the spectrum never comes "down", and the two are not resolvable using the Cole-Cole fit), by "Cb" or "Cc". A "c" spectra with very small real component variation is typical of an unaltered igneous rock, or a relatively fresh sedimentary rock, and is given an "n" ("null") classification. Criteria for evaluating spectra can be readily programmed into a small computer, after which evaluation can be done in a relatively objective and systematic fashion. Examples of all the described types of spectra are included in this paper, along with the Zonge and Cole-Cole parameterization, and are tabulated in Table 2.

The plotting convention for the Argand diagrams in this paper are all with the negative imaginary axis in the "up" direction. This is because virtually all linear rock spectra are of a dispersive nature, (i.e., energy-absorptive) and all therefore plot in the negative imaginary direction, or negative phase direction if plotted in polar coordinates. The Argand diagram representation was chosen by the author in this paper because it combines both real and imaginary (amplitude and phase) information in the same curve, and shows more clearly the subtle variations in the rock behavior. This convention has the disadvantage of amplifying the noise in the data, however, but this is also valuable information in the author's opinion.

TABLE 2. Cole-Cole and Zonge model curve-fit parameters, for the complex resistivity electrical spectra, and spectral letter-classifications shown in the paper.

FIGURE	LABELED	SPECTRAL CLASSIFICATION SYMBOL	COLE-COLE PARAMETERS	ZONE PARAMETERS	DESCRIPTION
14	171_K_76	CA	R_o=1.05±0.0047 M=0.957±0.0022 τ= 0.44±0.75E-2 C=0.646±0.0052		Serpentinized Harzburgite (See Table 1)
14	38_S_76	cC	R_o=0.977±0.0076 M=926±1714 τ=0.96E-12±0.47E-11 C-0.39±0.014		Serpentinized Harzburgite (See Table 1)
14	SC_2_76	C	R_o-1.206±0.045 M=0.994±0.658 τ=0.29E-6±0.25E-5 C-0.129±0.042		Dunite with Disseminated Chromite (See Table 1)
14	SC_4_76	AC	R_o=1.166±0.072 M_1=0.206±0.054 τ_1=4.21E+2±8.56E+2 C_1=0.238±0.041 M_2=5.19±14.2 τ_2=0.55E-7±0.32E-6 C_2=0.516±0.036		Dunite with Disseminated Chromite (See Table 1)
14	P_7_76	bC	R_o=1.147±0.064 M_1=219.7±245.5 τ_1=0.27E-10±0.67E-10 C_1=0.477±0.039 M_2-0.215±0.061 τ_2=0.125E+3±0.416E+3 C_2=0.144±0.051		Serpentinized Dunite with Disseminated Chromite (See Table 1)
15	6_PE_74	CAC	R_o=1.231±0.074 M_1=0.281±0.046 τ_1=0.14E+3±0.174E+3 C_1=0.288±0.030 M_2=99.9±183.2 τ_2=0.35E-8±0.11E-7 C_2=0.617±0.017		Massive Chromite (See Table 1)
15	BLD_BRM	N	R_o=1.038±0.011 M=0.460±0.29 τ=0.96E-6±1.01E-6 C=0.126±0.084		Massive Chromite from Brown's Mine
24	BFD_R10X4	Cb	R_o=1.313±0.059 M=0.67±0.063 τ=0.29E-1±0.88E-2 C=0.148±0.021	CDL-3.67 E-4 RCT=2.01 AK=0.139 RDC=1.06 AN=0.052	Field Data- Brown's Mine
24	BFD_R-2X1	A	R_o+1.61±0.814 M=0.969±0.797 τ=0.80E-3±0.83E-2 C=0.057±0.074	CDL=2.39 E-4 RCT=3.00 AK=0.120 RDC=1.04 AN=0.084	Field Data- Brown's Mine
24	BFD_R7X3	C	R_o=1.223±0.077 M=0.667±0.174 τ=0.11E-2±0.24E-2 τ=0.11E-2±0.24E-2 C=0.132±0.039	CDL=3.03 E-4 RCT=2.75 AK=0.105 RDC=1.04 AN=0.083	Field Data- Brown's Mine
15	BLD_Z1516	Cb	R_o=1.018±0.0017 M_1=0.161±0.021 τ_1=0.180±0.031 C_1=0.445±0.021 M_2=0.872±0.714 τ_2=0.34E-5±0.99E-5 C_2=0.399±0.089	CDL=3.70 E-4 RCT=2.01 AK=0.101 RDC=1.01 AN=1.13	Massive Chromite from Brown's Mine
15	BLD_Z1515	CA	R_o=1.021±0.001 M=0.139±0.002 τ=0.158±0.006 C=0.361±0.007	CDL=0.269 E-4 RCT=5.38 AK=0.060 RCD=1.00 AN=0.068	Massive Chromite from Brown's Mine

Table 2 continued

19	RMFD_R8X2	Cc	R_o=1.051±0.020 M=0.270±0.119 τ=0.14E-3±0.52E-3 C=0.160±0.053	CDL=.275 E-4 RCT=7.73 AK=0.20 RCD=1.01 AN=0.011	Field Data- Red Mountain
15	RMLD_Z1508	CA	R_o=1.123±0.018 M_1=0.281±0.163 τ_1=3.542±0.917 C_1=0.379±0.084 M_2=0.433±0.837 τ_2=0.67E-4±0.52E-3 C_2=0.279±0.401	CDL=7.65 E-4 RCT=1.05 AK=0.372 RCD=1.04 AN=0.73	Massive Chromite from the Red Mountains Outcrop
16	RMLD_Z1507	C	R_o=1.192±0.017 M=1.078±0.093 τ=0.97E-4±0.95E-4 C=0.143±0.010	CDL=13.5 E-4 RCT=1.04 AK=0.255 RDC=1.04 AN=0.60	Serpentinized Dunite from the Red Mountain Outcrop
16	RMLD_Z1504	C	R_o 1.035±0.002 M=0.663±0.024 τ=0.61E-3±0.14E-3 C=0.274-0.006	CDL=4.33 E-4 RCT=1.92 AK=0.074 RDC=0.99 AN=0.016	Serpentinized Harzburgite from the Red Mountain Outcrop
24	BFD_ROX2	n	R_o=1.062±0.025 M=0.405±0.263 τ=0.78E-5±0.54E-4 C=0.145±0.55	CDL=1.14 E-4 RCT=7.86 AK=0.036 RDC=1.01 AN=0.042	Field Data- Brown's Mine

FIGURE CAPTIONS

Figure

1. Idealized ophiolite section, showing the position of the chromite pods, from Dickey, 1975.
2. Idealized model of a podiform chromite deposit.
3. Location of the Josephine ultramafic complex, and the areas referred to in this paper.
4. Specific gravity as a function of serpentine content and also chromite content for samples collected in the Josephine complex. An asymptotic behavior of specific gravity as a function of the degree of serpentinization can be clearly observed (outline).
5. Porosity as a function of serpentine content and of chromite content for samples collected in the Josephine complex. Most of the higher percent serpentine samples show a lower porosity than the massive chromite samples.
6. Magnetic susceptibility as a function of serpentine content and also chromite content for samples collected in the Josephine complex. Chromite samples generally have low magnetic susceptibility, whereas, susceptibility shows a nearly exponential relationship with percent serpentine, though with wide scatter.
7. Compressional seismic velocity for dry rock samples as a function of chromite content and also of olivine content for samples collected in the Josephine complex. (Chromite content does not appear to correlate with velocity in these measurements, but insufficient massive chromite samples are represented. Olivine-rich rocks, or those having small amounts of serpentinization, showed consistently high velocities.

8. Compressional seismic velocities for dry-rock samples as a function of serpentine content for samples collected in the Josephine complex. An asymptotic relationship can be observed where high serpentine content means lower velocity in the rock.
9. Spectral reflectance from visible wavelengths to the far infra-red for several arch-typal rock samples (natural surfaces unless otherwise indicated) from the Josephine complex, from Hunt and Wynn, (1979). It appears from this figure that harzburgite can be distinguished from dunite with a 5/6 or 5/7 LANDSAT image ratio, whereas chromite could be distinguished by its low albedo. The samples are in the right-hand column.
10. Resistivities of several serpentinized and unserpentinized rocks from the Josephine complex. There is an apparent lack of correlation between resistivity and percent chromite or percent serpentine.
11. Relationship between resistivity and porosity for the samples from the Josephine complex. Even in semi-log form, this figure shows wide scatter in the expected results, suggesting that there are non-pore-fluid conductivity mechanisms substantially involved in the rock suite. (Pore-fluid is controlled at 100 ohm-meters.)
12. Phase-angle shift between transmitted and received signal for several chromite-bearing rock samples form the Josephine complex. The phase-shift is for a transmitted current sine-wave of 0.1 Hz., and shows a moderate polarization for samples of massive chromite, but unusually high polarization for samples having high magnetic susceptibility (and therefore probably clinochrysotile-rich?).

13. Phase-angle shift for serpentinized and unserpentinized rocks from the Josephine complex, showing an apparent lack of correlation with percent serpentine in the rocks.

14. Complex resistivity electrical spectra (Argand diagrams) for several arch-typal dunite and harzburgite samples from the Josephine complex. Frequencies from 0.01 to 1000. Hz. were used, and magnitude-phase data were transformed into the Cartesian complex plane for plotting purposes to enhance spectral variations for visual examination. Real and imaginary components were normalized by the magnitude of the real component at 0.01 Hz. Original data are solid lines, Cole-Cole fit done with triangles; see the text for further explanation of plotting and interpreting these curves. In these spectra, the dunites appear to be separable from the harzburgites. These and all subsequent spectra are listed in Table 2.

15. Complex resistivity electrical spectra for several arch-typal massive chromite samples from Brown's Mine and the Red Mountain outcrop, showing the characteristic "peaked" or "bent" spectral behavior described in the text. Data are solid lines, Cole-Cole fit done with triangles, Zonge equation fit done with squares.

16. Complex resistivity electrical spectra for two samples of peridotite from the Red Mountain outcrop: These spectra are characteristic of peridotites that have been substantially (40 percent) serpentinized. Data are solid lines, Cole-Cole fit done with triangles, Zonge equation fit done with squares.

17. Geophysical traverses over the chromite outcrops at the Red Mountain site, southern extreme of the Josephine complex. A: Topography, unexaggerated scale, chromite outcrops shown with hachurs. Spacing

between station numbers is 10 m. B: Total - field magnetics profile, showing a magnetic low delimited by highs over the outcrops. C: VLF-EM apparent-resistivity profile, showing resistive highs over both outcrops.

18. Geophysical traverses over the chromite outcrops at the Red Mountain site, Josephine complex. A: Topography. B: Dipole-dipole apparent-resistivity pseudosection, values in ohm-meters, showing resistivity highs at each outcrop. The eastern outcrop has caused a modified "pants leg" shape of 500 Ω-m. separated by the single station in the 200 Ω-m. range. C: Dipole-dipole phase-angle pseudosection, values in milliradians for 0.1 Hz., showing a moderate phase-angle anomaly going to depth beneath the western (larger) outcrop of chromite. Spacing between station numbers is 10 m.

19. Geophysical traverse over the chromite outcrops at the Red Mountain site, Josephine complex. A: Topography. B: Complex resistivity spectral-type pseudosection, showing a "Cc" spectral shape anomaly beneath each outcrop, going to depth beneath the western one. C: Example spectral-types used to compile the pseudosection in B from field data, showing "C" and "Cc" spectral types.

20. Seismic field records taken over the westernmost (larger) chromite outcrops at the Red Mountain site, Josephine complex. Each trace is for a single geophone, spaced 2 m apart, with the topmost traces being from the east side of the outcrop. A very pronounced velocity increase shows up at the chromite outcrop, seen here as a bulge in first-arrival times between traces 16 and 26, caused by a much shortened arrival time during this interval. The shot-point (source) is located 4 m to the east (top of sheet) of the #4 geophone trace. A vertical compressional source 1/2-m deep was used.

21. Seismic field records taken over the westernmost chromite outcrop at the Red Mountain site, Josephine complex. The only difference between figures 20 and 21 is the location of the shot-point. Figure 21 is the reverse-direction analog of figure 20, with the shot-point (source) being located 4 m to the west of the #12 (bottom of page) geophone-trace. The chromite shows up again as a bulge in arrival times, in this case between traces 4 and 14.

22. Geophysical traverses at Tyson's mine, south-central part of the Josephine complex. A: Topography and geology, scale not exaggerated, showing inferred location of the chromite pod. B. Total-field magnetic profile, showing a 500 nT low over the chromite deposit. C: VLF-EM apparent-resistivity profile, values in ohm-meters, showing unusually low resistivities in the serpentinite.

23. Geophysical traverses over the chromite deposit at Brown's Mine, central part of the Josephine complex. A: Topography, unexaggerated scale, showing the inferred location of the orebody. There is a gentle 15-degree eastern dip in the foliation of pyroxene-rich zones in the harzburgite mass. B: Dipole-dipole apparent-resistivity pseudosection, values in ohm-meters, showing the strong effects of serpentine at each end. C: Dipole-dipole phase-angle pseudosection, values in milliradians for 0.1 Hz., showing an anomalous feature in the center at the 45 milliradian point. Spacing between station numbers is 60 m.

24. Complex resistivity spectral-types from the field data collected over the Brown's Mine target, Josephine complex. These spectra are the arch-types of the letter designations that are plotted in figure 25 and discussed in the text.

25. Geophysical traverses over the chromite deposit at Brown's Mine, Josephine complex. A: Complex resistivity spectral-type pseudosection, showing the "Cb" shape apparently pin-pointing the chromite deposit below the center of the line. B: Total-field magnetic profile, showing the strong effects of serpentine, partially masking a possible low over the chromite deposit. C: Topography.

26. Ground - magnetic profile at Brown's Mine, Josephine complex. A: Unfiltered profile, same as figure 25B. B: Filtered profile, with difference filter applied and wavelengths less than 60 m removed, showing a magnetic low over the chromite deposit.

Idealized Ophiolite Section

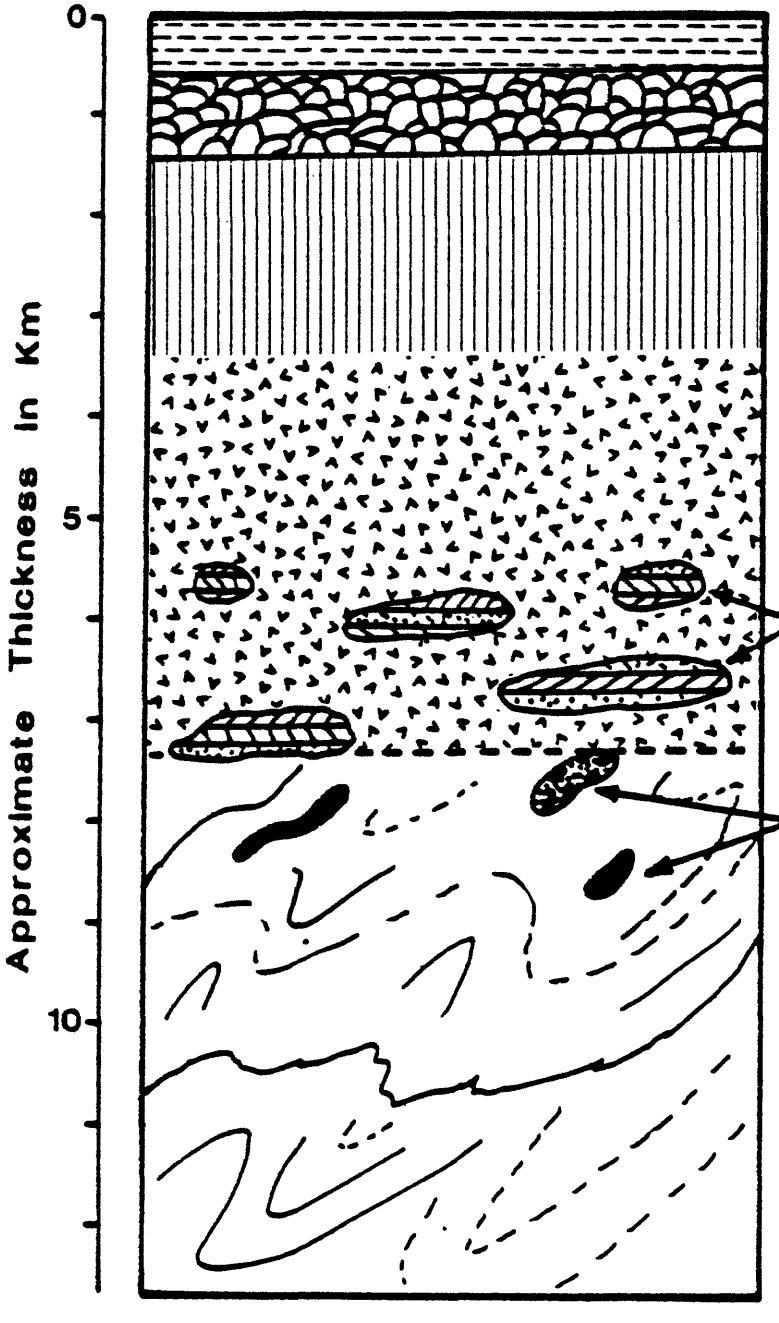

After Dickey [1975]

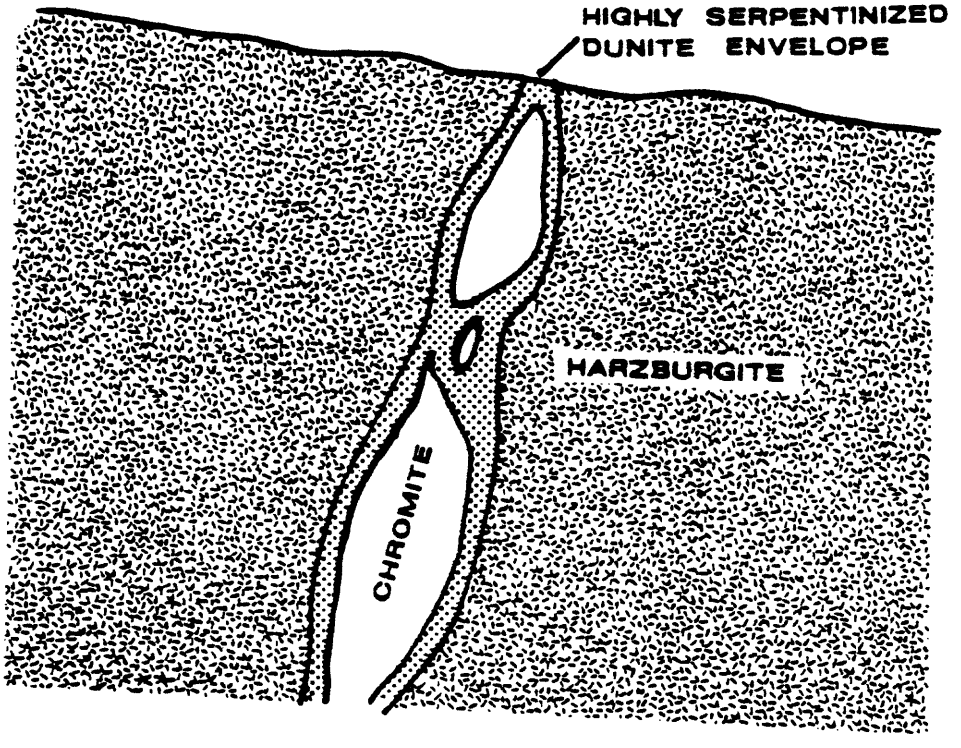
HIGHLY SERPENTINIZED
DUNITE ENVELOPE
HARZBURGITE
CHROMITE

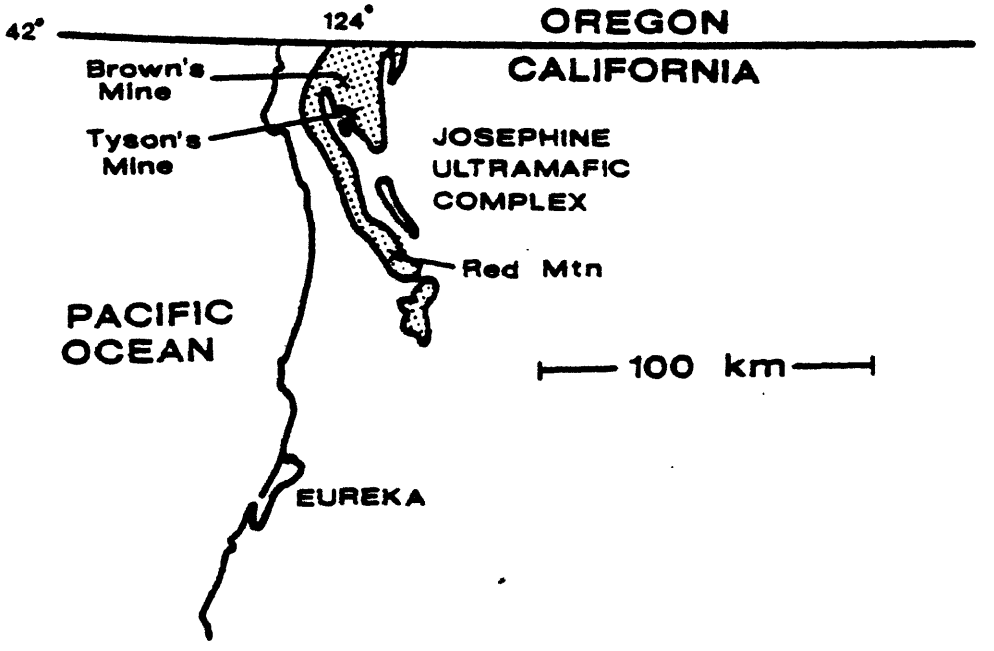
42°
124°
OREGON
CALIFORNIA
Brown's Mine
Tyson's Mine
JOSEPHINE ULTRAMAFIC COMPLEX
Red Mtn
PACIFIC OCEAN
100 km
EUREKA

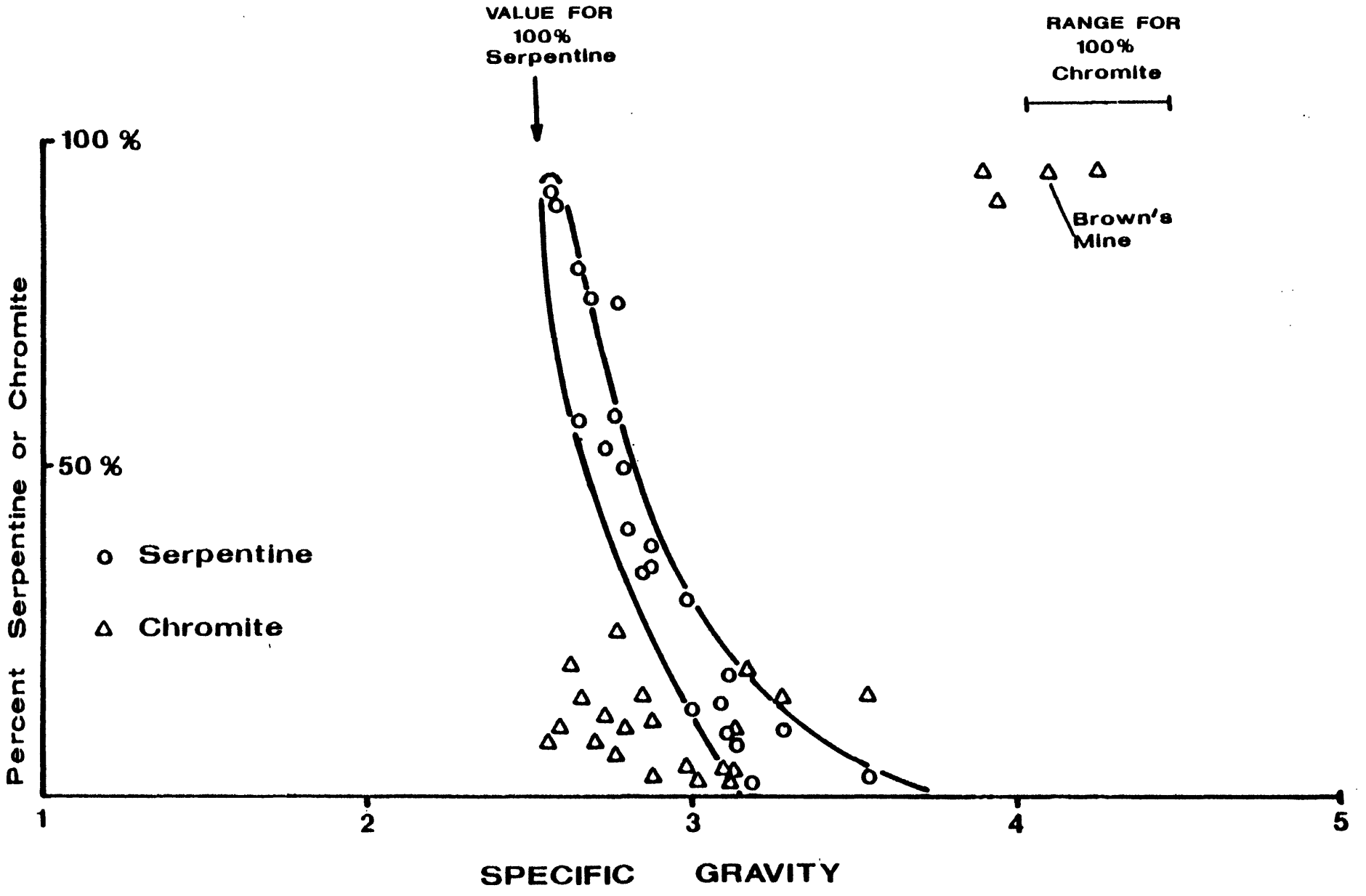
VALUE FOR
100%
Serpentine
RANGE FOR
100%
Chromite
Brown's
Mine
100 %
50 %
Percent Serpentine or Chromite
o Serpentine
Δ Chromite
1
2
3
4
5
SPECIFIC GRAVITY

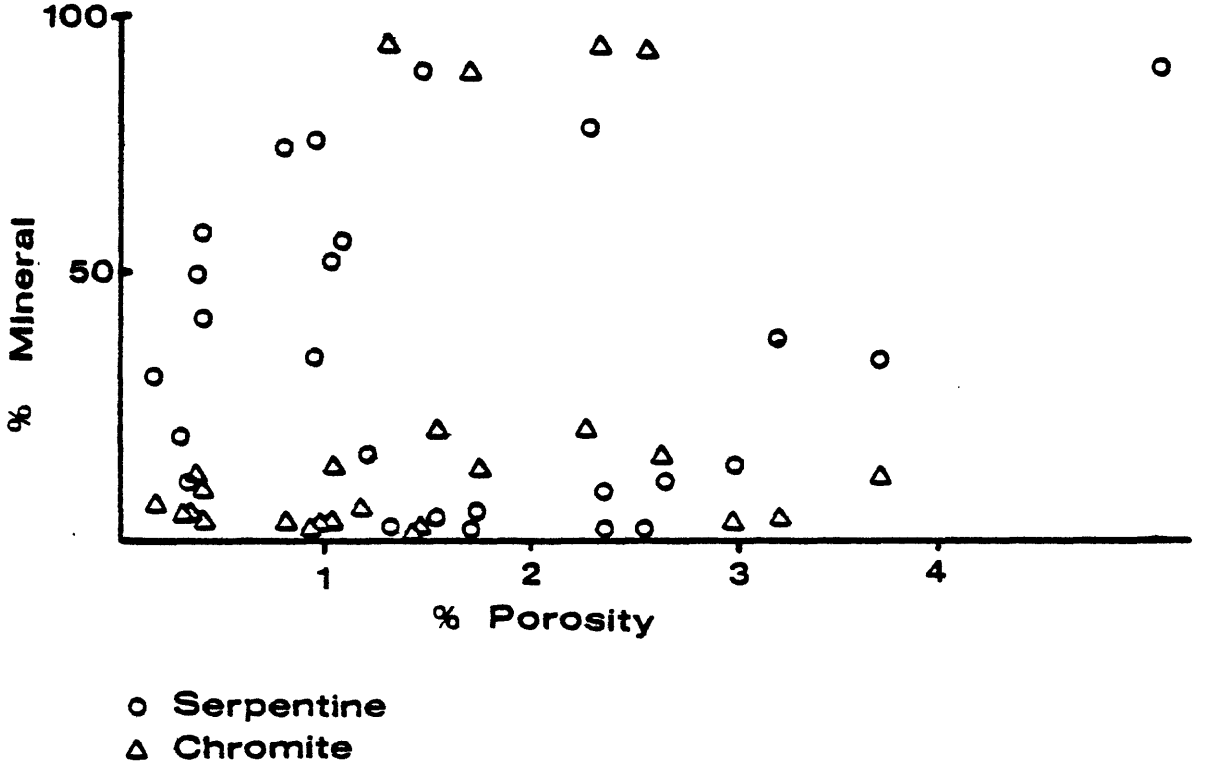
100
50
% Mineral
1
2
3
4
% Porosity
o Serpentine
Δ Chromite

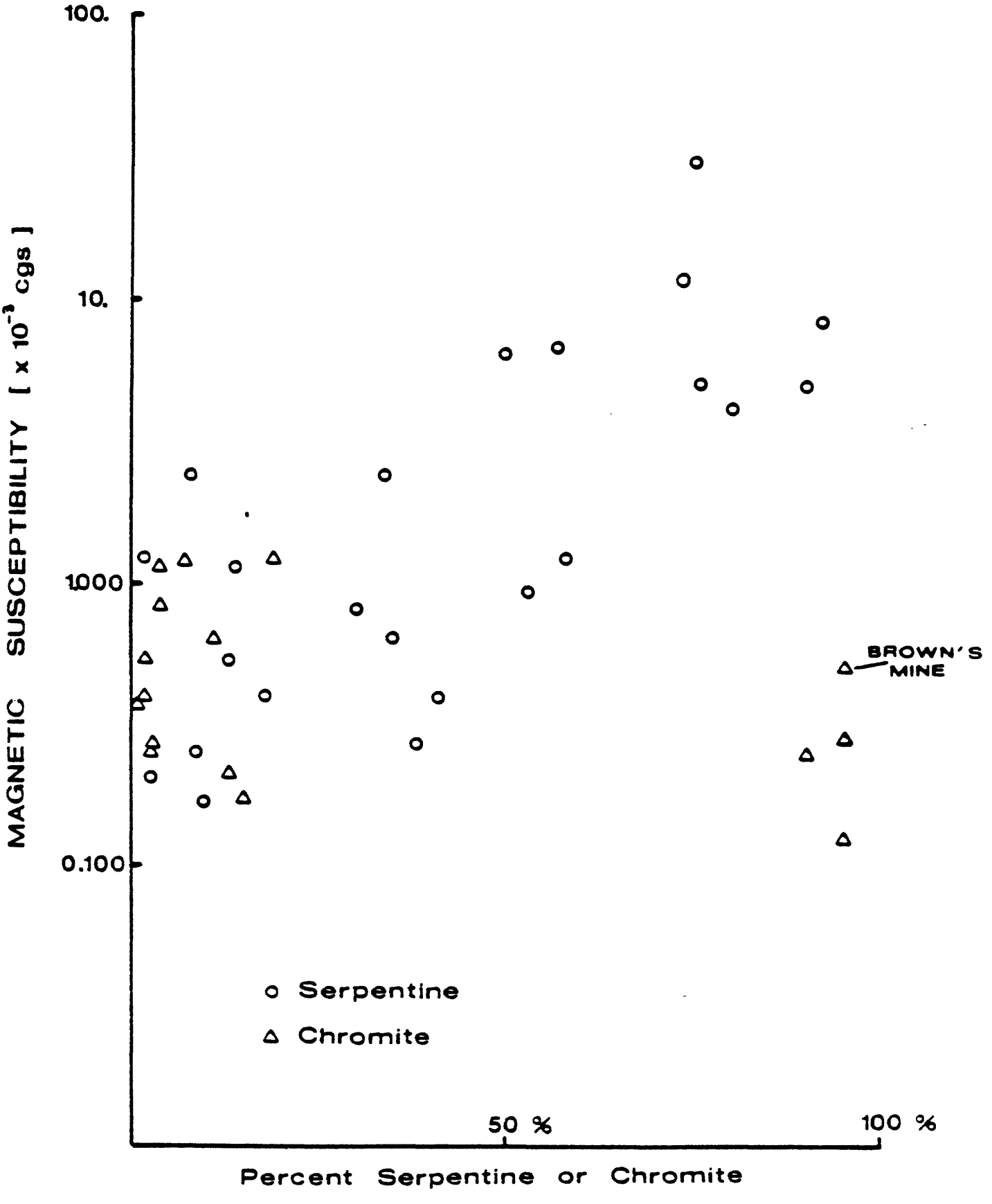
100.
10.
1.000
0.100
MAGNETIC SUSCEPTIBILITY [x 10⁻³ cgs]
BROWN'S MINE
Serpentine
Chromite
50 %
100 %
Percent Serpentine or Chromite

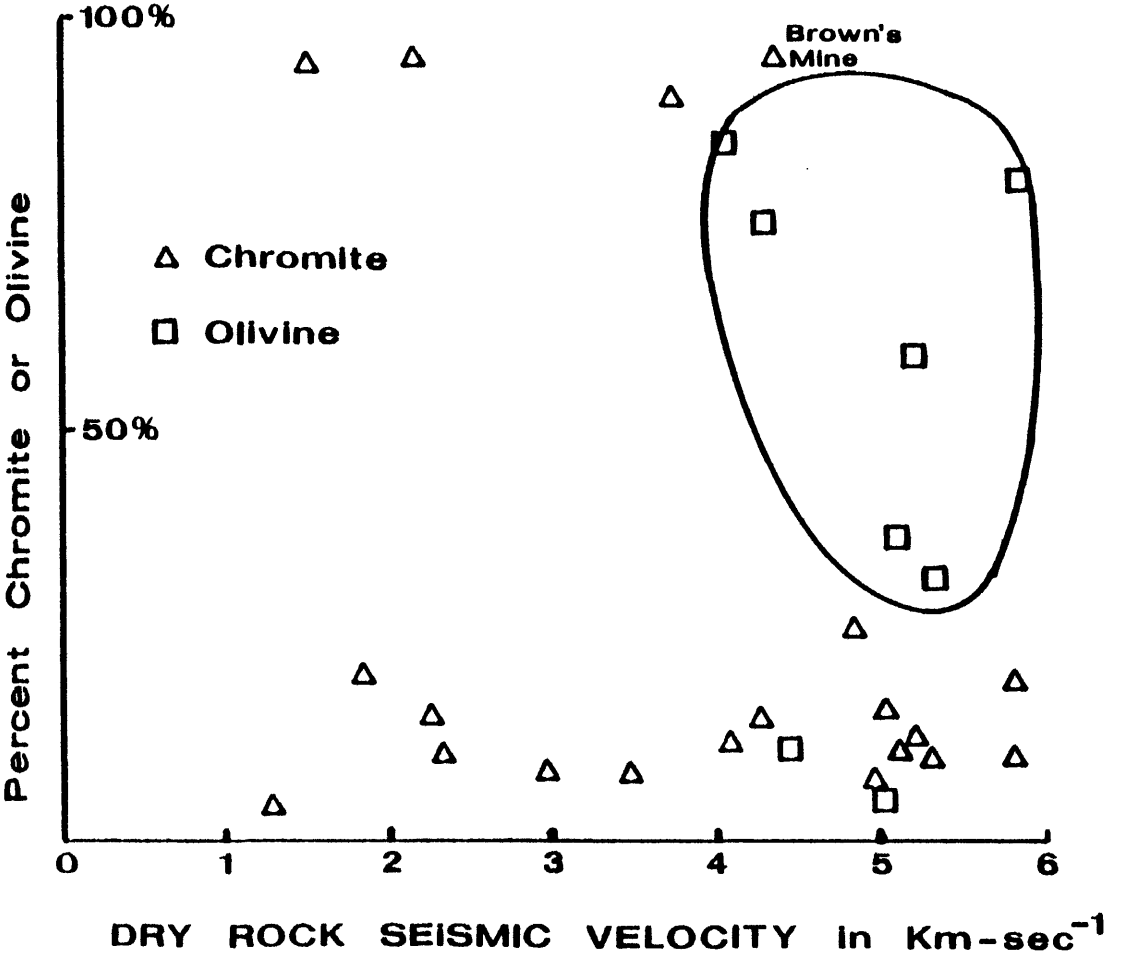
100%
50%
Brown's Mine
Chromite
Olivine
Percent Chromite or Olivine
0
1
2
3
4
5
6
DRY ROCK SEISMIC VELOCITY in Km-sec^{-1}

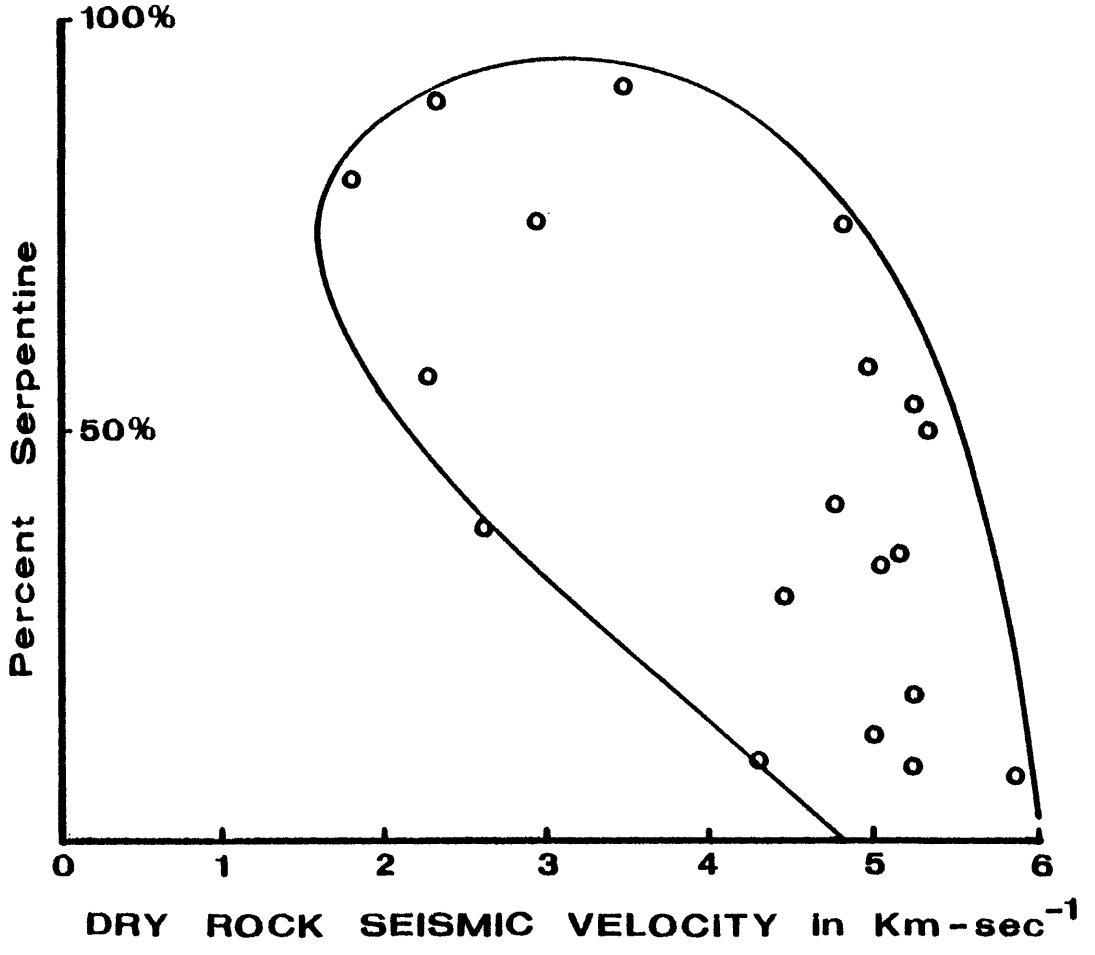
100%
50%
Percent Serpentine
0
1
2
3
4
5
6
DRY ROCK SEISMIC VELOCITY in Km-sec^{-1}

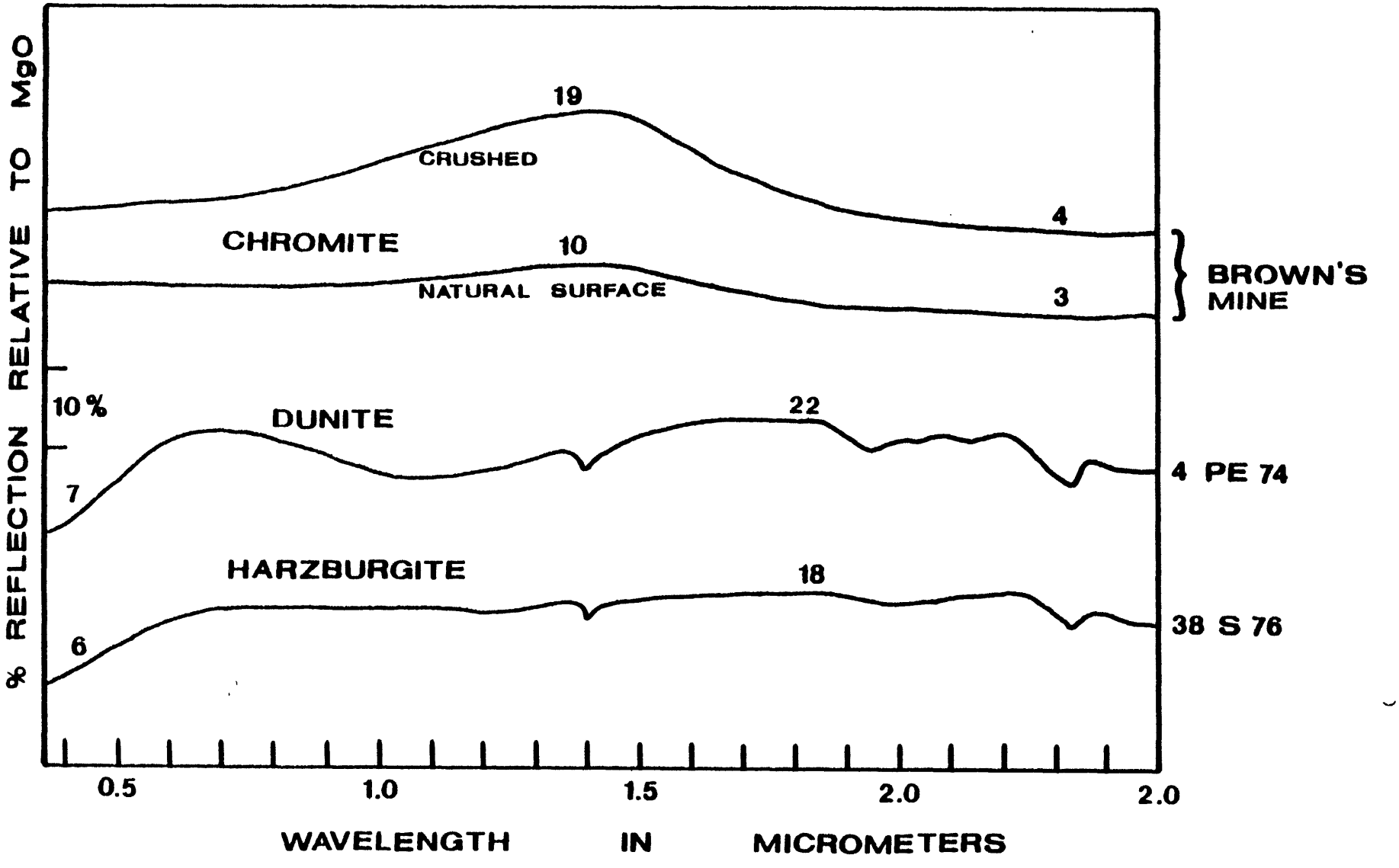

From Hunt & Wynn [1979]

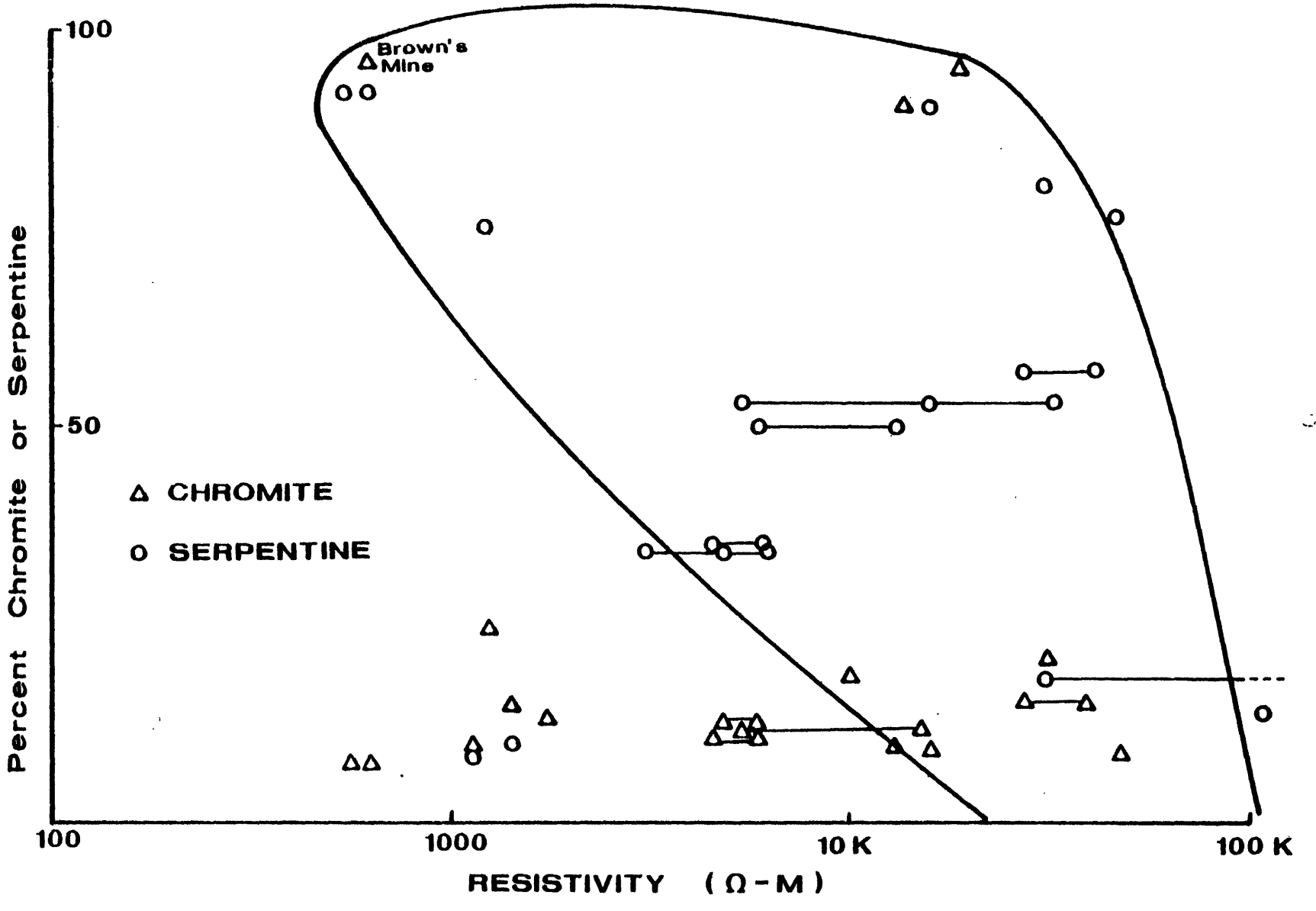
100
50
Brown's Mine
Δ CHROMITE
o SERPENTINE
Percent Chromite or Serpentine
100
1000
10 K
100 K
RESISTIVITY (Ω - M)

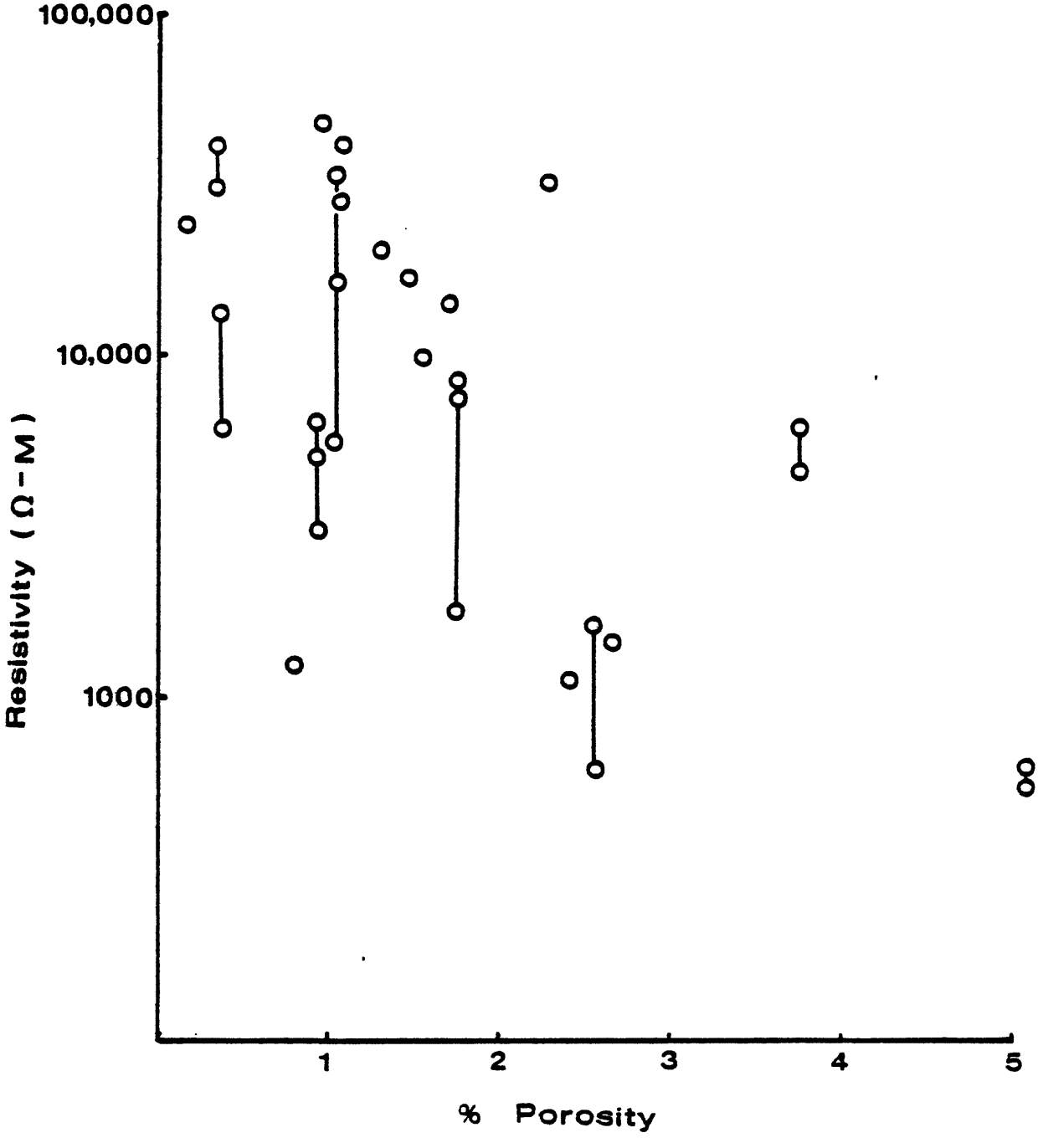
100,000
10,000
1000
Resistivity (Ω-M)
1
2
3
4
5
% Porosity

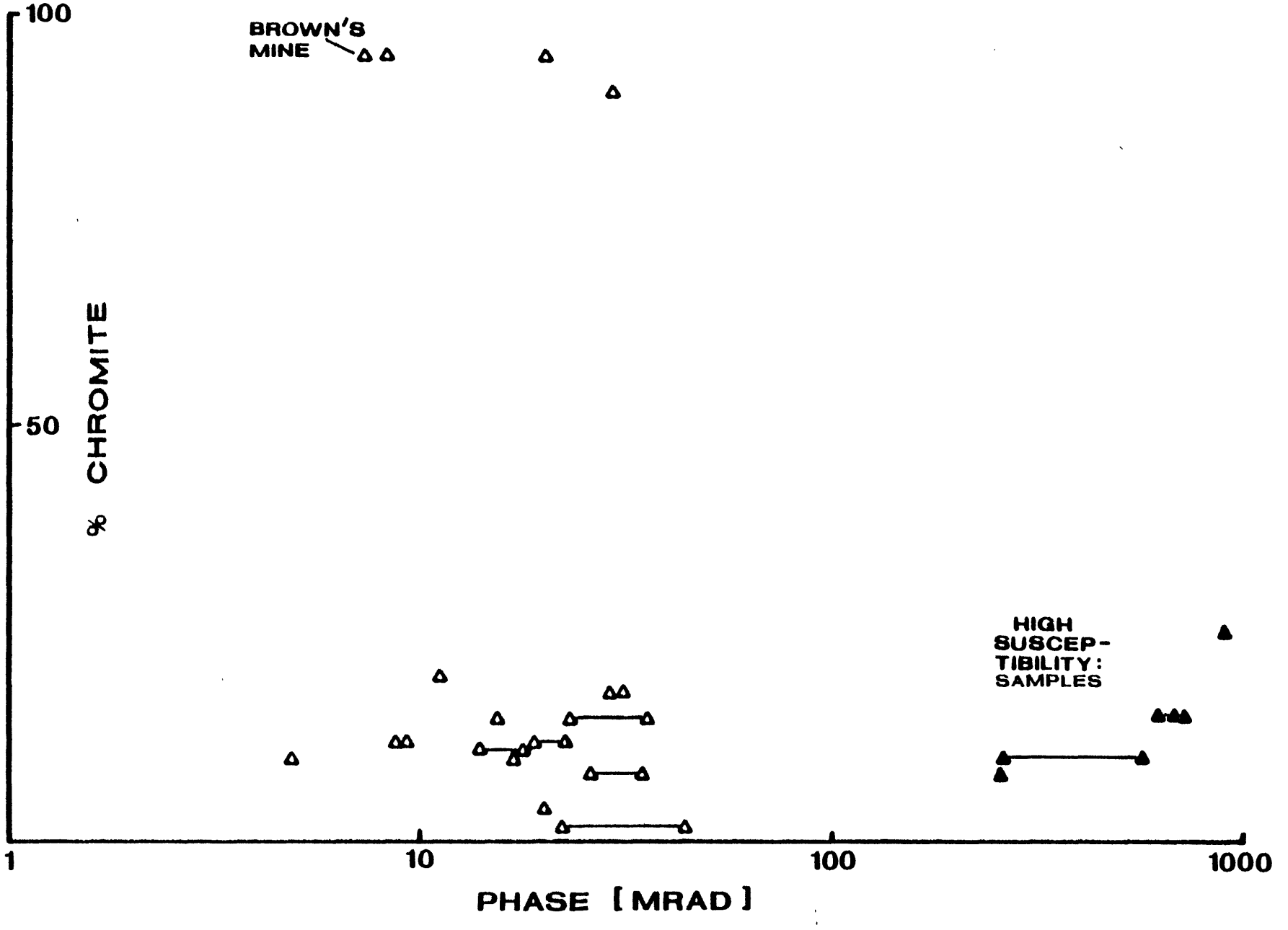
100
50
% CHROMITE
BROWN'S MINE
HIGH SUSCEP-TIBILITY: SAMPLES
1
10
100
1000
PHASE [MRAD]

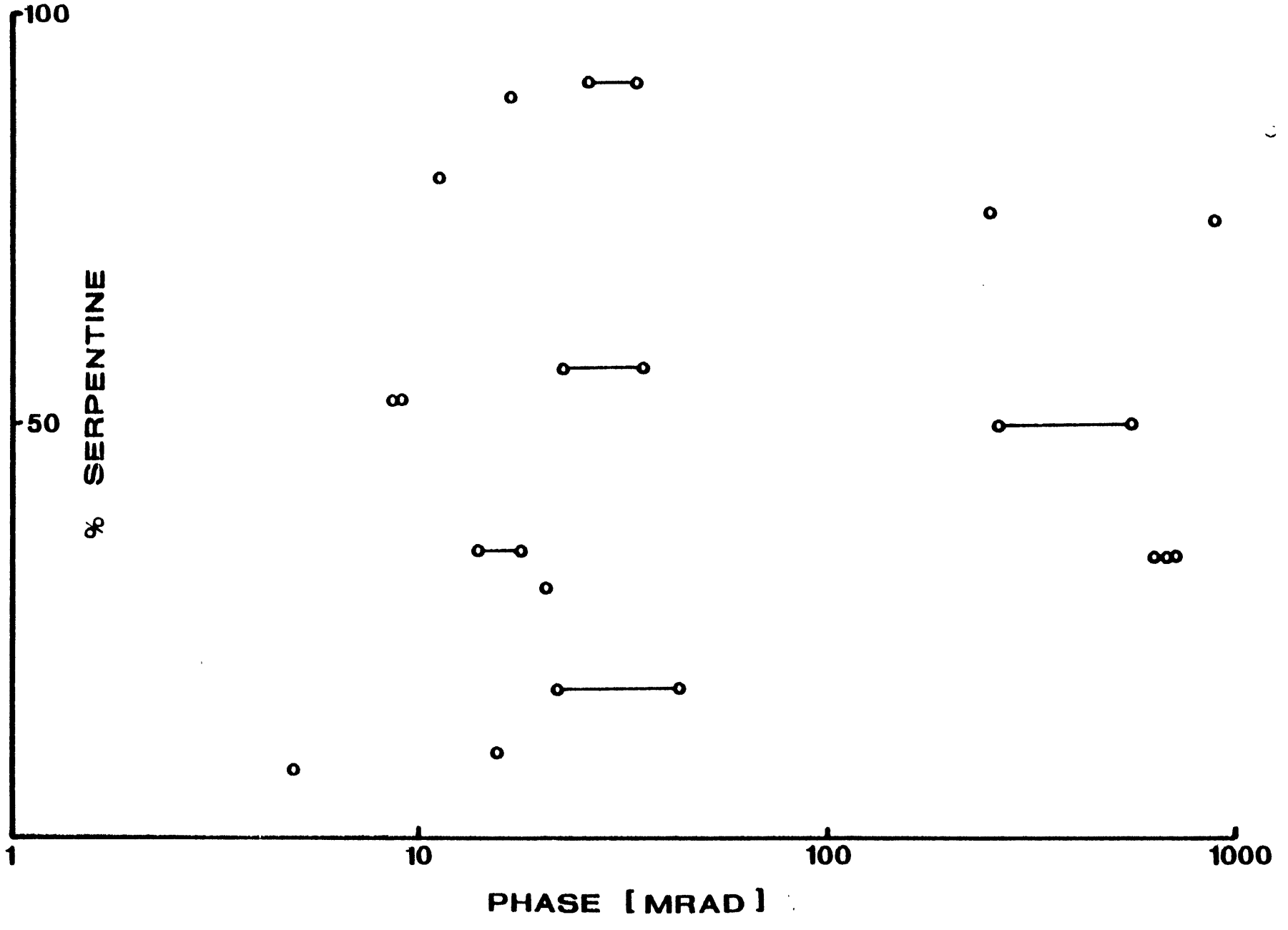
100
50
% SERPENTINE
1
10
100
1000
PHASE [MRAD]

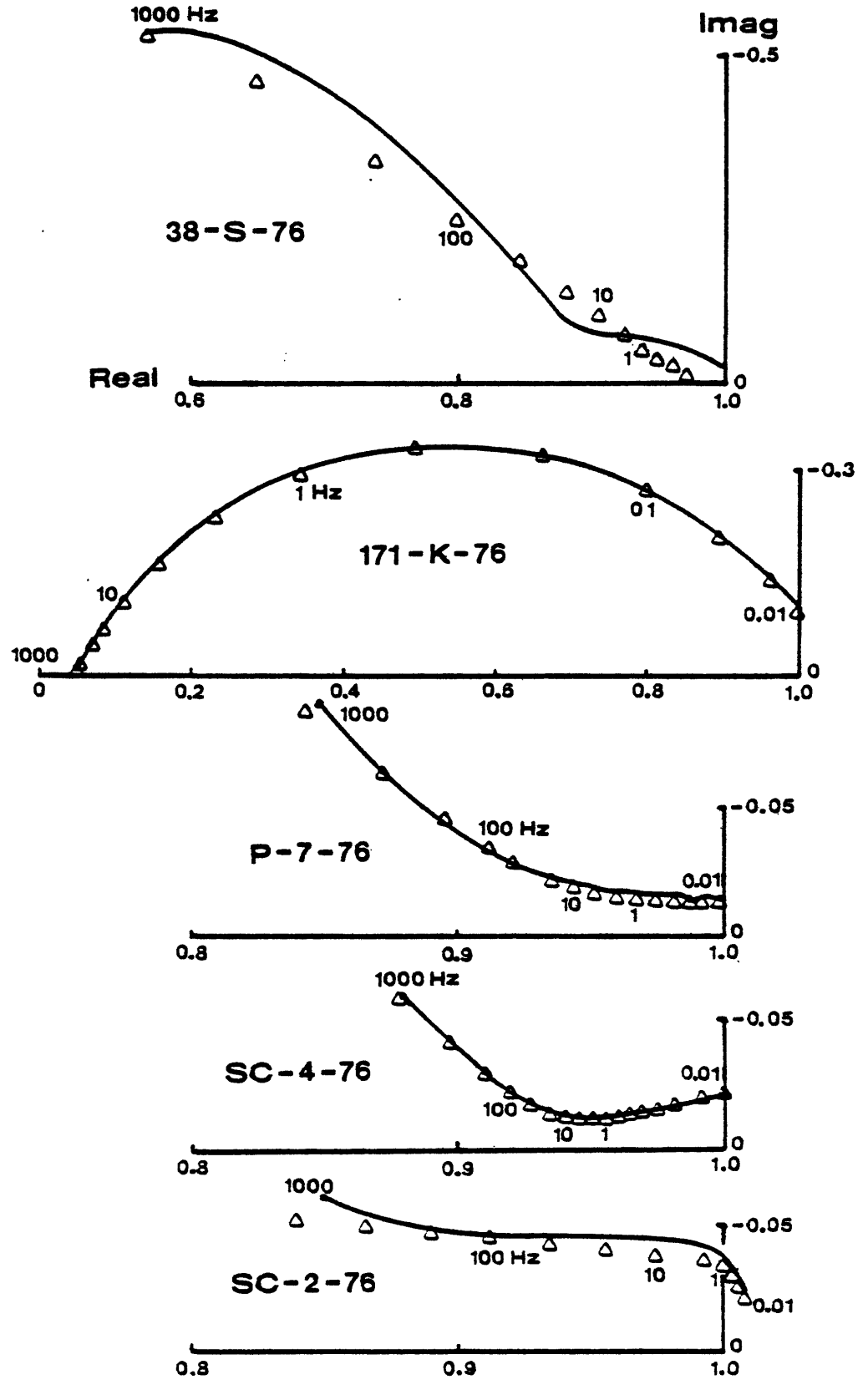
1000 Hz
Imag
-0.5
38-S-76
100
10
1
Real
0.6
0.8
1.0
0
1 Hz
-0.3
171-K-76
10
1000
0.01
0
0.2
0.4
0.6
0.8
1.0
1000
100 Hz
P-7-76
-0.05
0.01
10
1
0.8
0.9
1.0
1000 Hz
SC-4-76
100
10
1
1000
100 Hz
SC-2-76

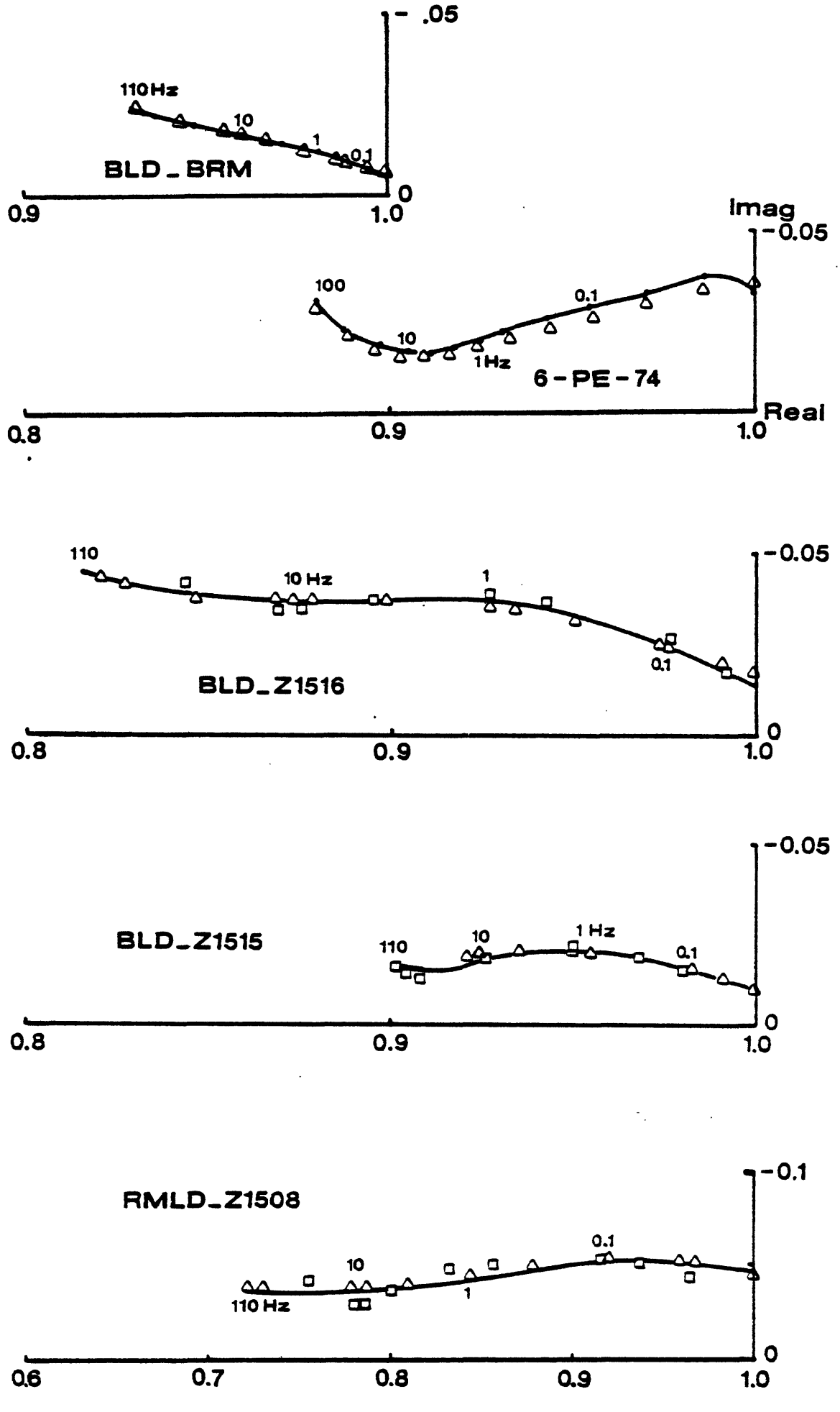
- .05
110Hz
10
1
0.1
BLD_BRM
0
0.9
1.0
Imag
-0.05
100
10
1Hz
0.1
6-PE-74
Real
0.8
0.9
1.0
110
10 Hz
1
0.1
-0.05
BLD_Z1516
0
0.8
0.9
1.0
-0.05
BLD_Z1515
110
10
1 Hz
0.1
0
0.8
0.9
1.0
-0.1
RMLD_Z1508
0.1
10
110 Hz
1
0
0.6
0.7
0.8
0.9
1.0

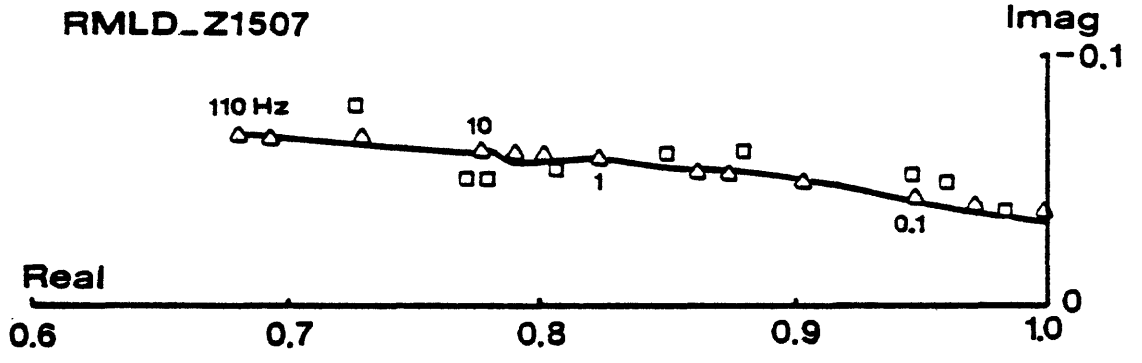
RMLD_Z1507
Imag
-0.1
110 Hz
10
1
0.1
Real
0
0.6
0.7
0.8
0.9
1.0

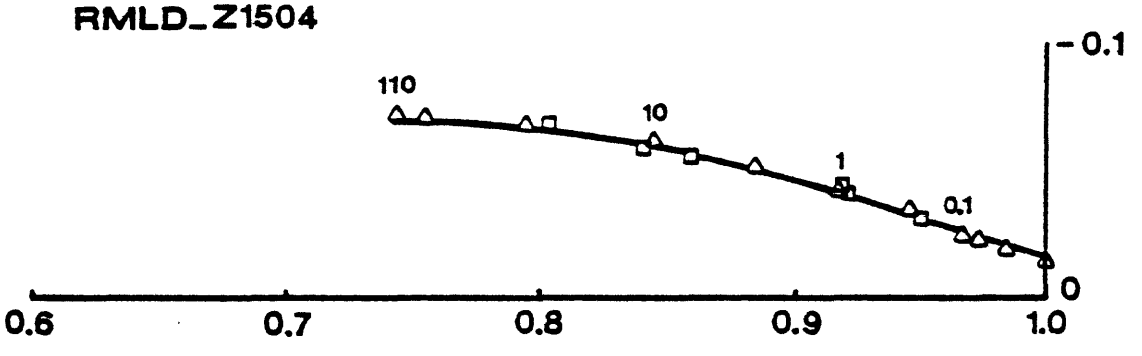
RMLD_Z1504
-0.1
110
10
1
0.1
0
0.6
0.7
0.8
0.9
1.0

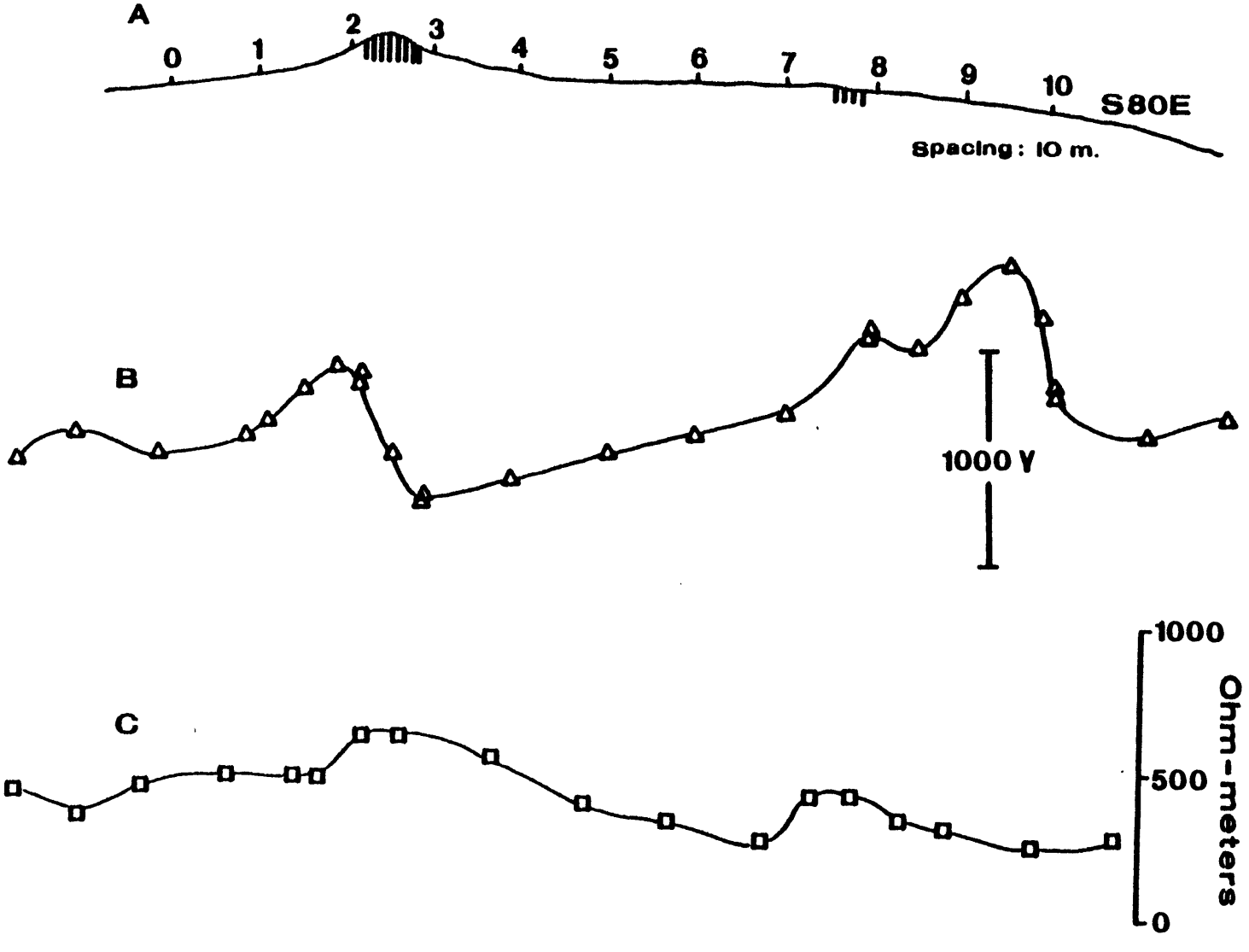
A
0
1
2
3
4
5
6
7
8
9
10
S80E
Spacing : 10 m.
B
1000 V
C
1000
500
0
Ohm-meters

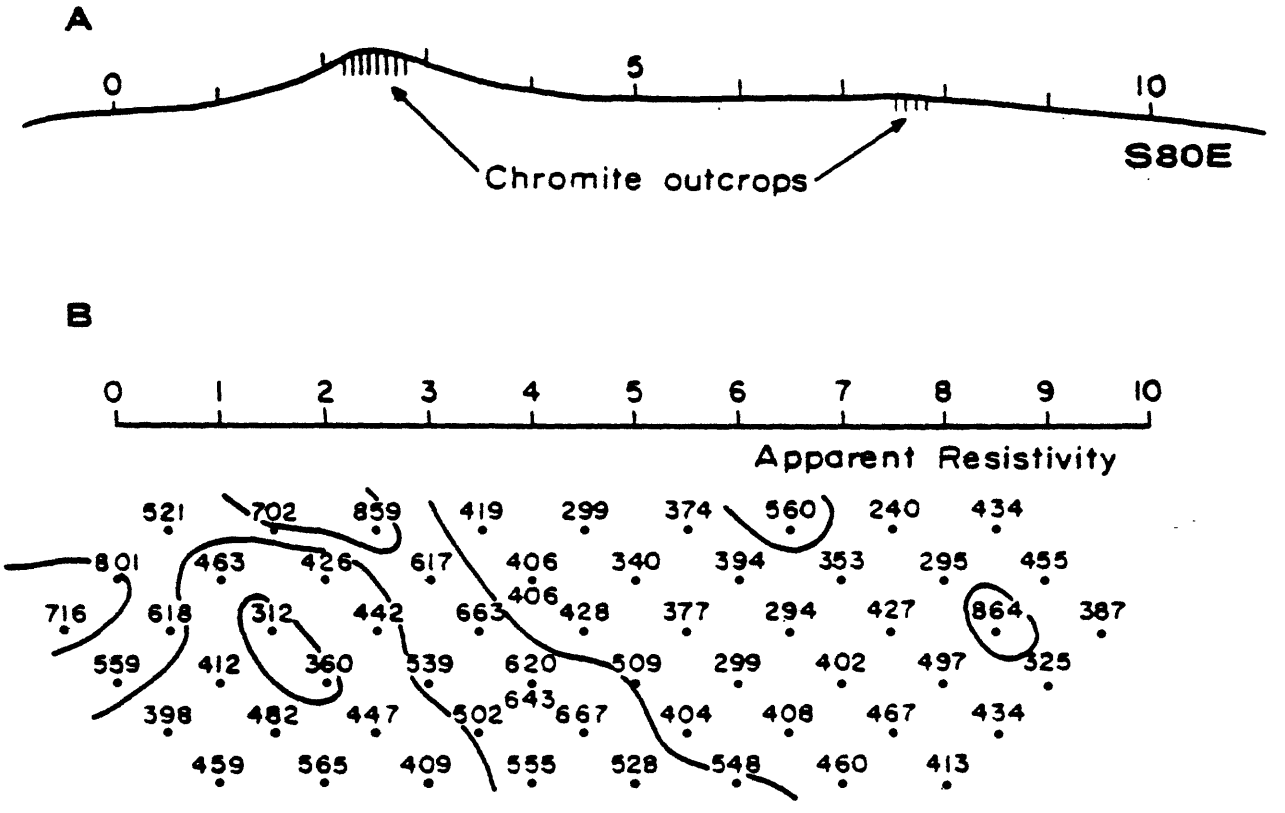
A
0
5
10
Chromite outcrops
S80E
B
0 1 2 3 4 5 6 7 8 9 10
Apparent Resistivity
521 702 859 419 299 374 560 240 434
801 463 426 617 406 340 394 353 295 455
716 618 312 442 663 406 428 377 294 427 864 387
559 412 360 539 620 509 299 402 497 325
398 482 447 502 643 667 404 408 467 434
459 565 409 555 528 548 460 413
C
Spacing = 10 m
0 1 2 3 4 5 6 7 8 9 10
0.1 Hz Phase Angle
9 10 11 9 8 9 10 6 11
9 6 9 9 7 7 6 7 9 11
8 7 8 10 9 7 7 6 6 9 9 10
6 9 10 11 8 6 6 7 9 9
6 10 10 10 9 8 7 7 8 9
8 11 10 10 8 8 8 9

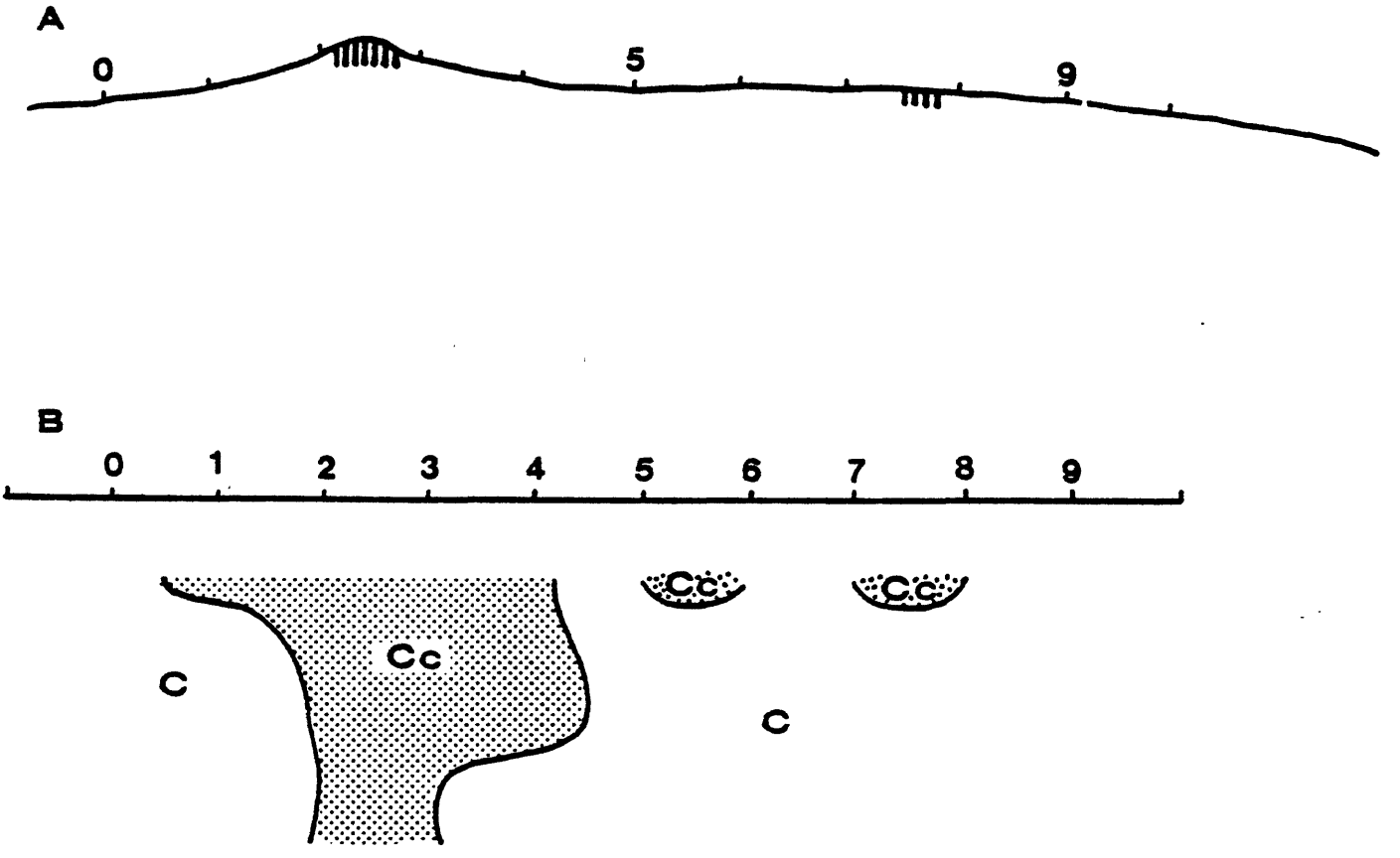
A
0
5
9
B
0 1 2 3 4 5 6 7 8 9
Cc
Cc
C
Cc
C

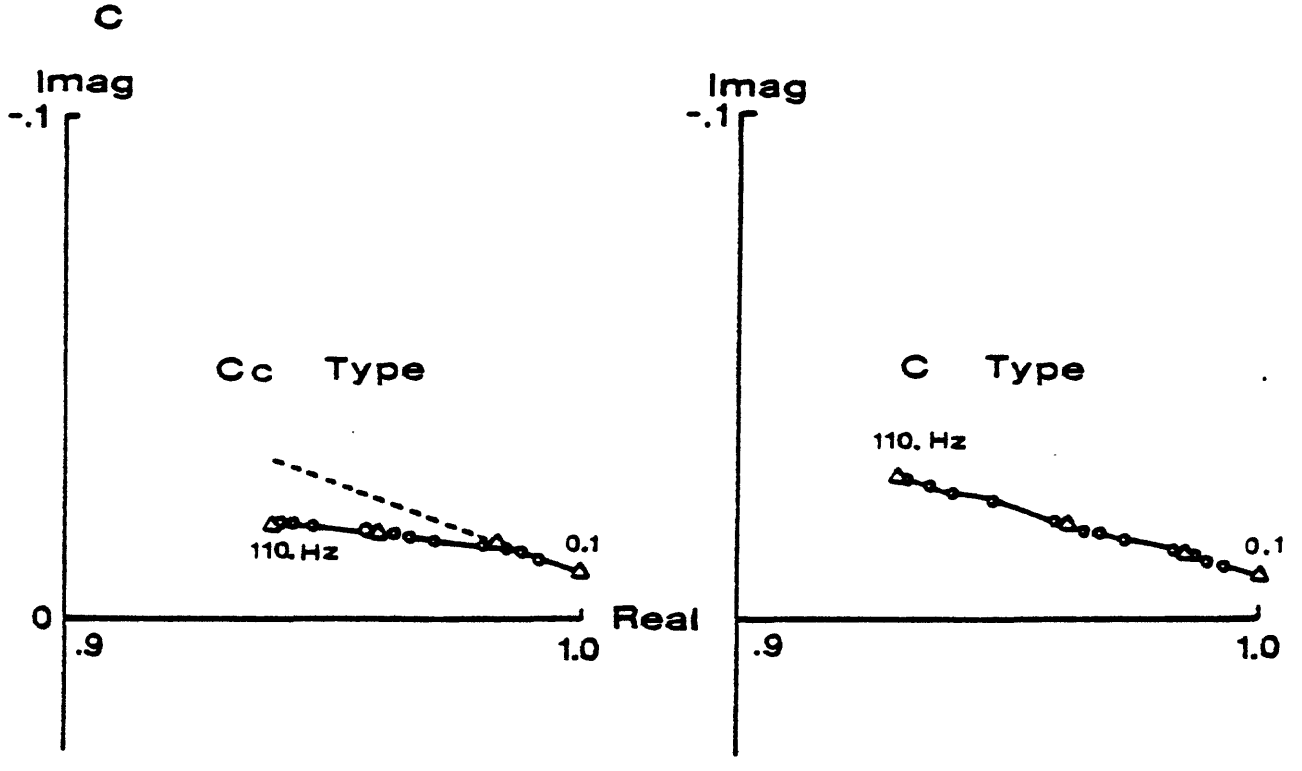
C
Imag
-.1
Cc Type
110. Hz
0.1
0
.9
1.0
Real
Imag
-.1
C Type
110. Hz
0.1
.9
1.0

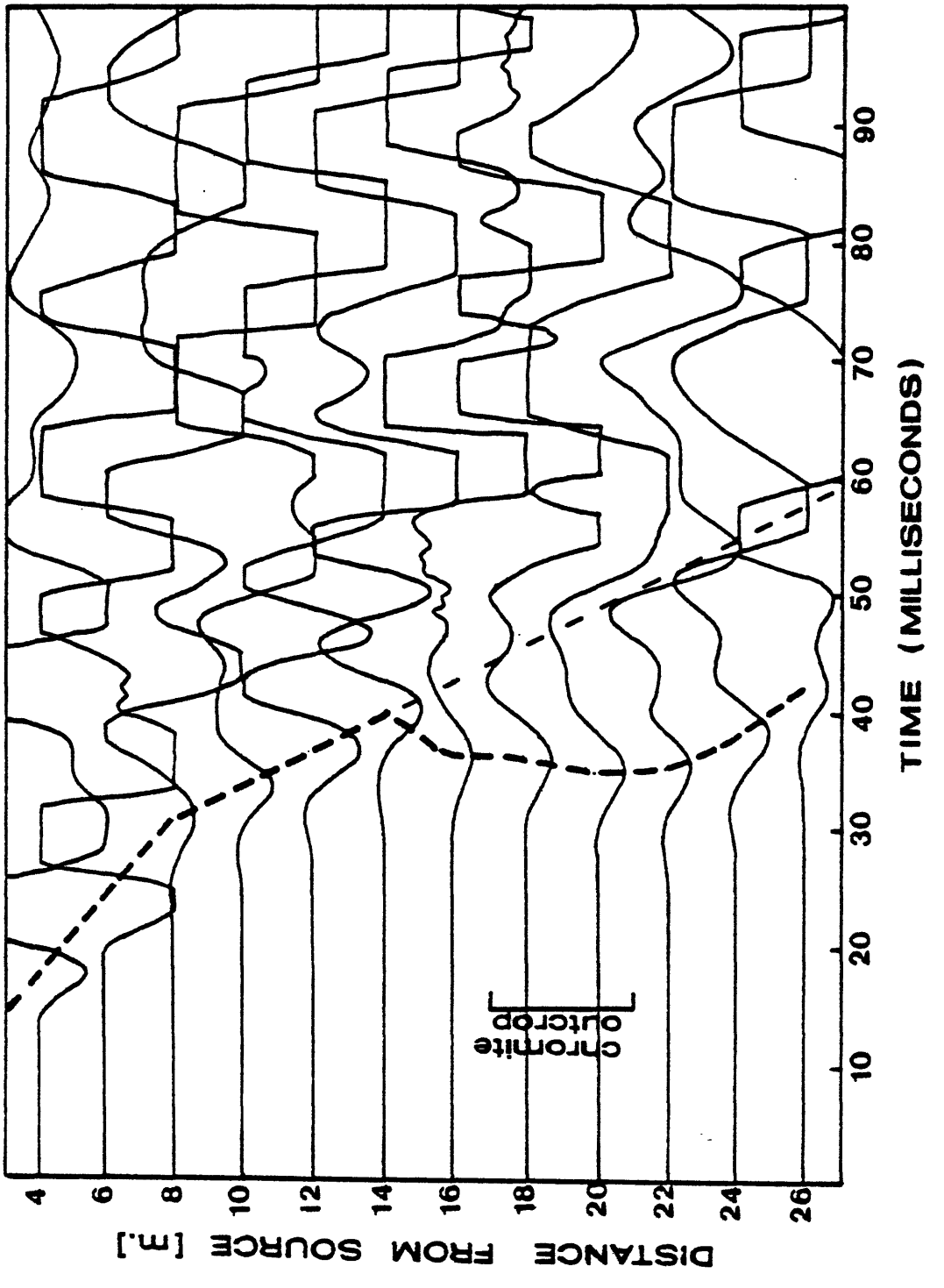
DISTANCE FROM SOURCE [m.]
4
6
8
10
12
14
16
18
20
22
24
26
chromite outcrop
10
20
30
40
50
60
70
80
90
TIME (MILLISECONDS)

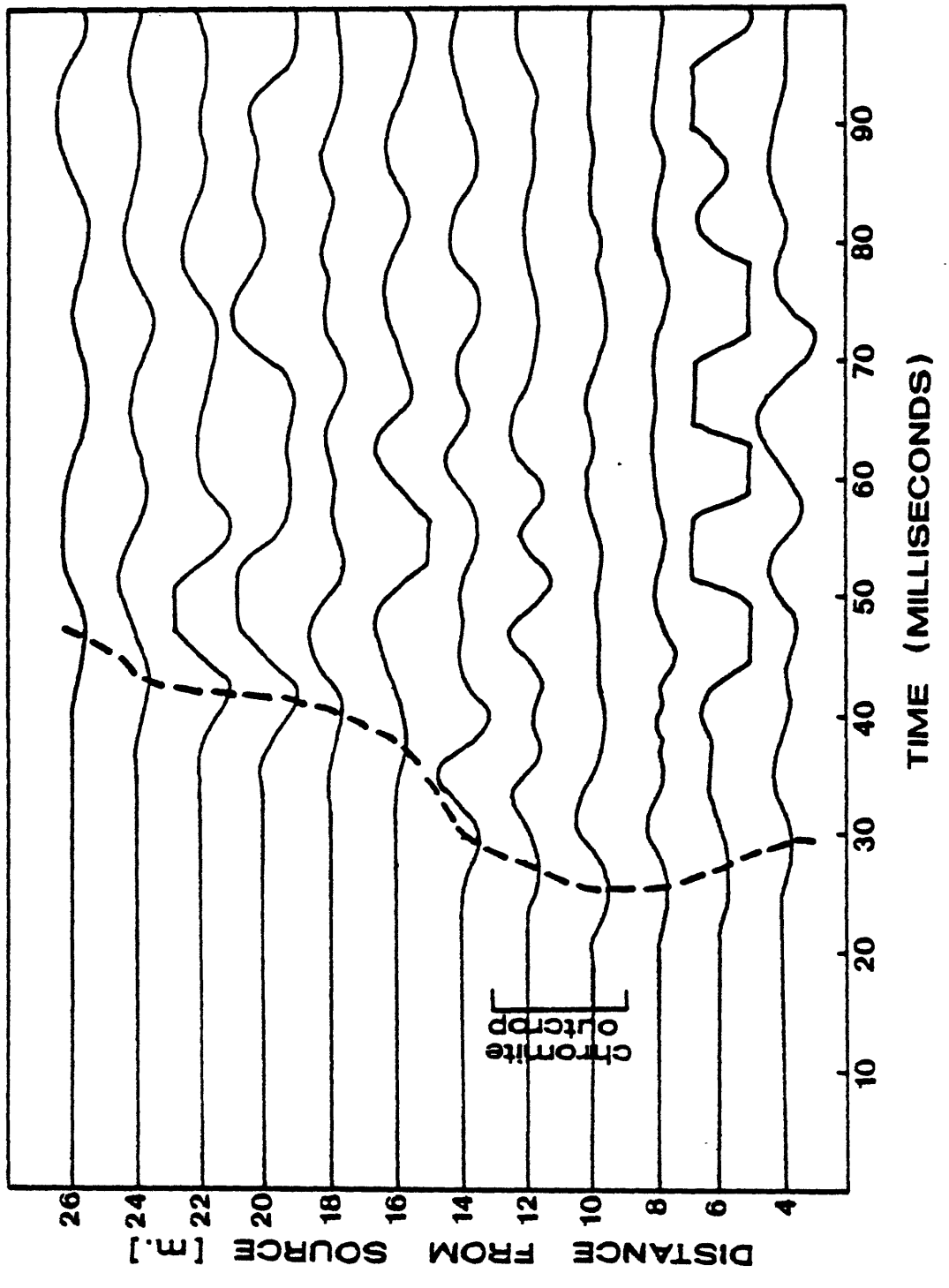
DISTANCE FROM SOURCE [m.]
26
24
22
20
18
16
14
12
10
8
6
4
TIME (MILLISECONDS)
10
20
30
40
50
60
70
80
90
chromite outcropp

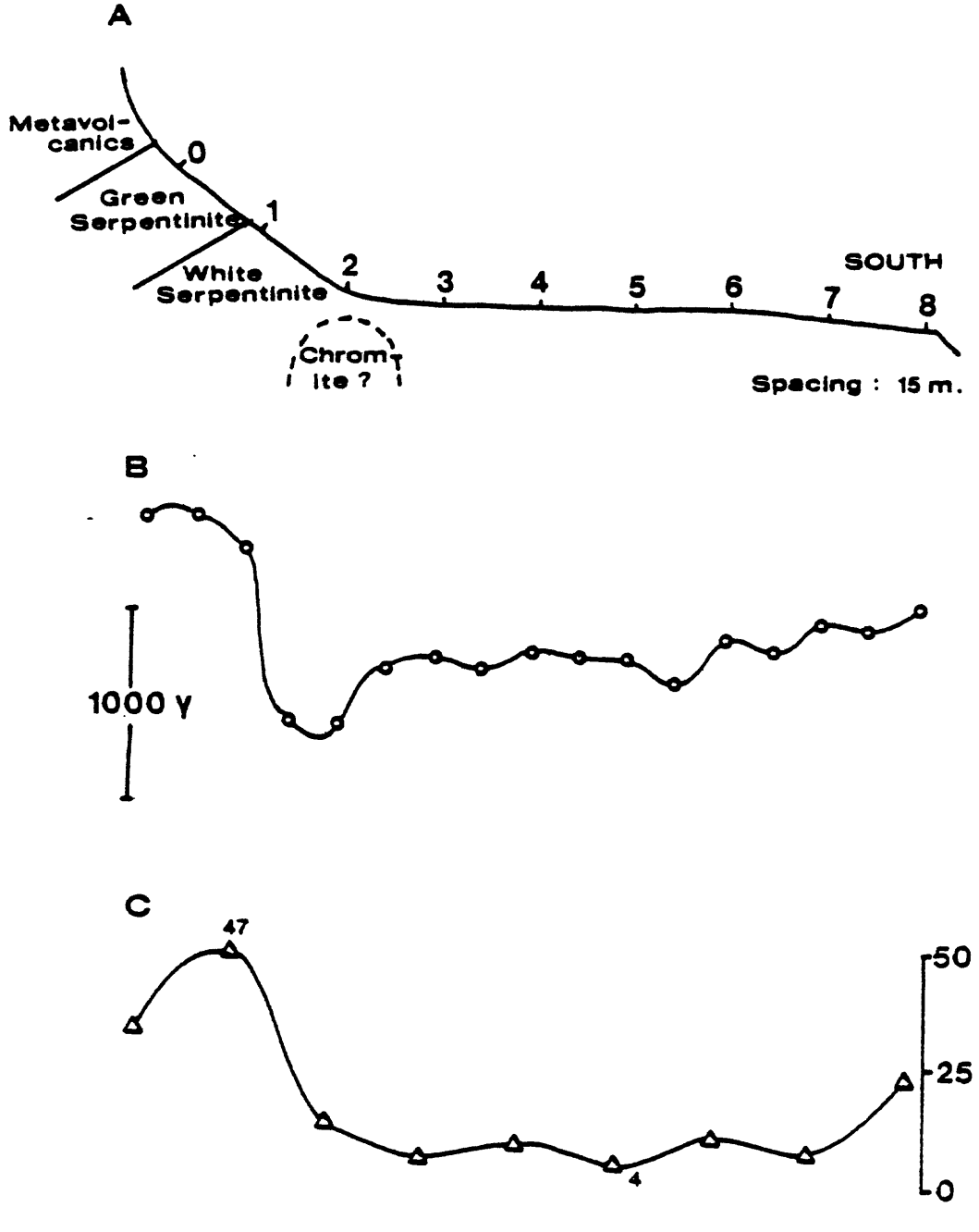
A
Metavol-
canics
0
Green
Serpentinite
1
White
Serpentinite
2
3
4
5
6
7
8
SOUTH
Chrom
ite ?
Spacing : 15 m.
B
1000 γ
C
47
4
50
25
0
Ohm-meters

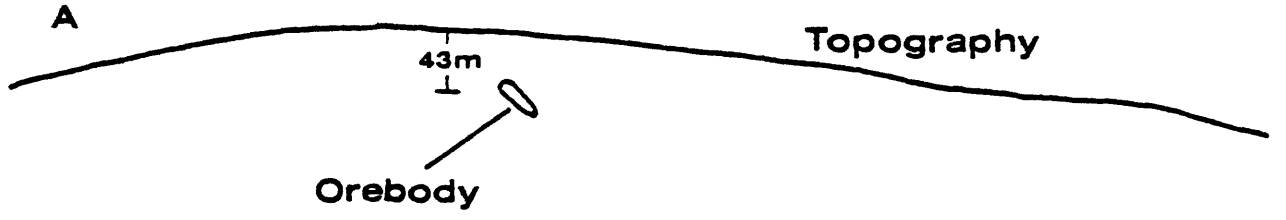
A
Topography
43m
Orebody

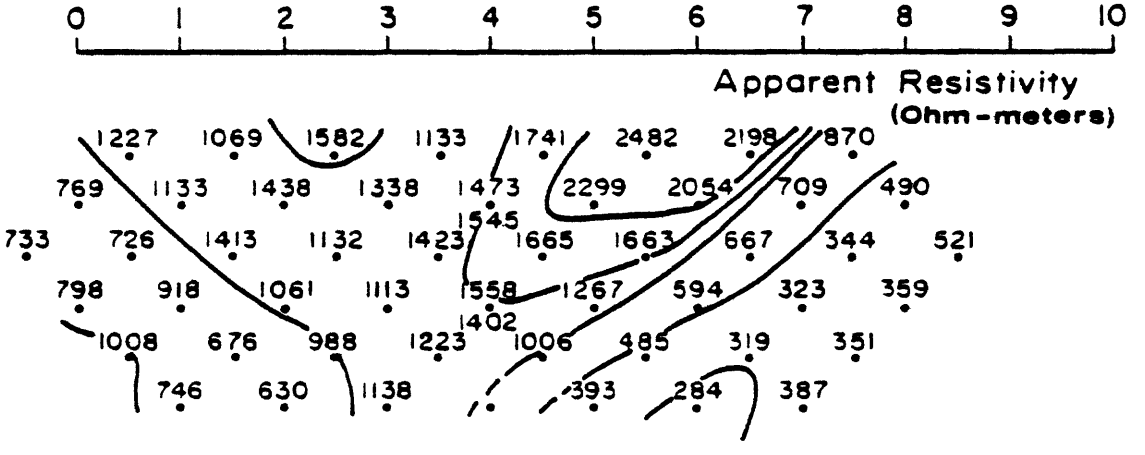
0 1 2 3 4 5 6 7 8 9 10
Apparent Resistivity
(Ohm-meters)
1227 1069 1582 1133 1741 2482 2198 870
769 1133 1438 1338 1473 2299 2054 709 490
1545
733 726 1413 1132 1423 1665 1663 667 344 521
798 918 1061 1113 1558 1267 594 323 359
1402
1008 676 988 1223 1006 485 319 351
746 630 1138 393 284 387

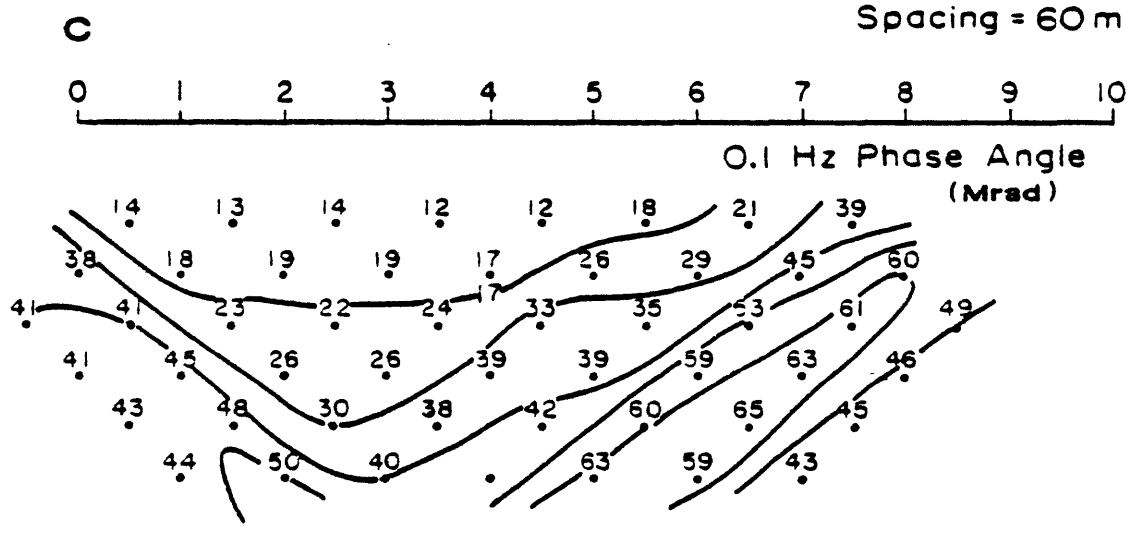
C
Spacing = 60 m
0 1 2 3 4 5 6 7 8 9 10
0.1 Hz Phase Angle
(Mrad)
14 13 14 12 12 18 21 39
38 18 19 19 17 26 29 45 60
41 41 23 22 24 17 33 35 53 61 49
41 45 26 26 39 39 59 63 46
43 48 30 38 42 60 65 45
44 50 40 63 59 43

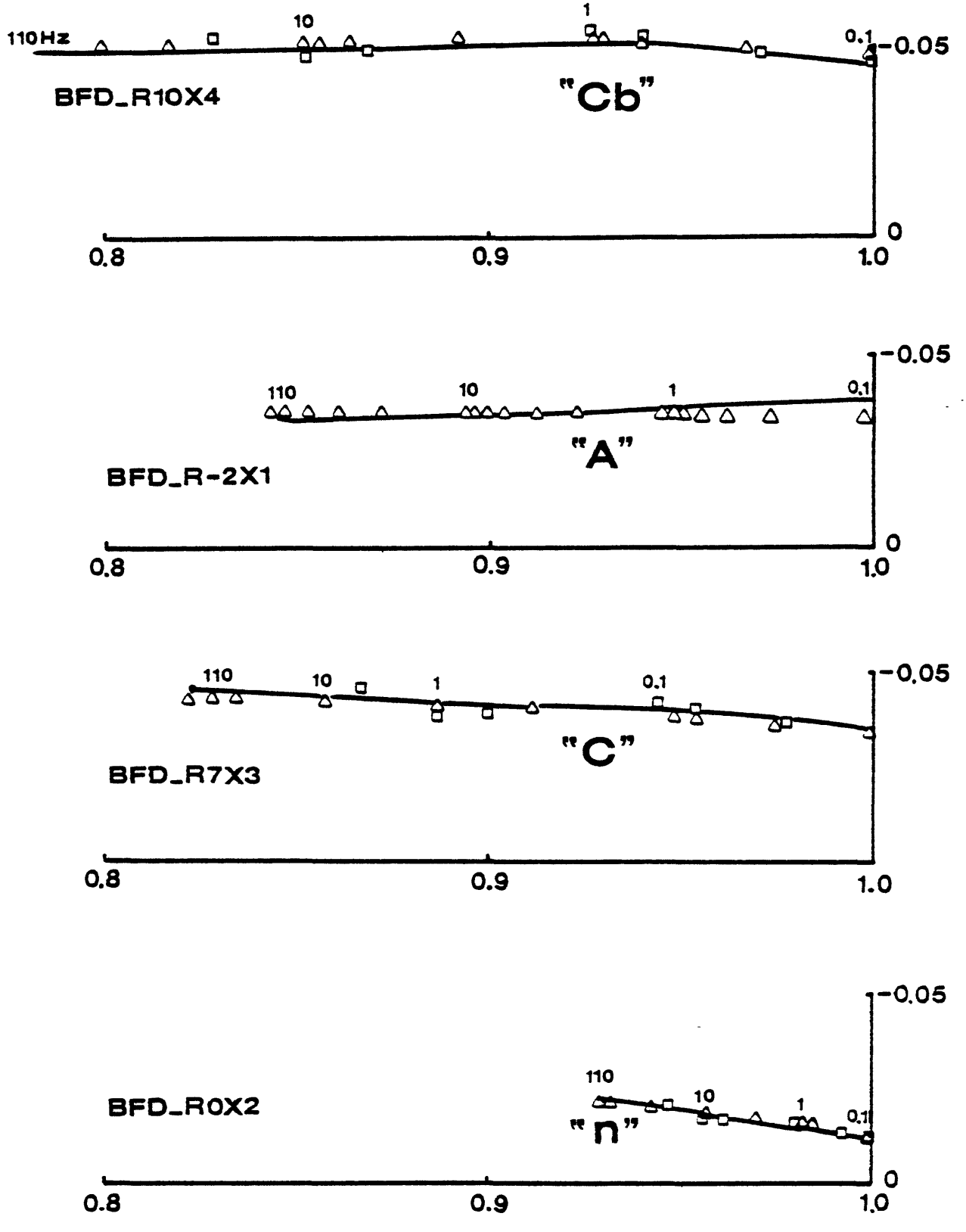
110Hz
10
1
0.1
-0.05
BFD_R10X4
"Cb"
0
0.8
0.9
1.0
110
10
1
0.1
-0.05
"A"
BFD_R-2X1
0
0.8
0.9
1.0
110
10
1
0.1
-0.05
"C"
BFD_R7X3
0.8
0.9
1.0
-0.05
110
10
1
0.1
BFD_R0X2
"n"
0
0.8
0.9
1.0

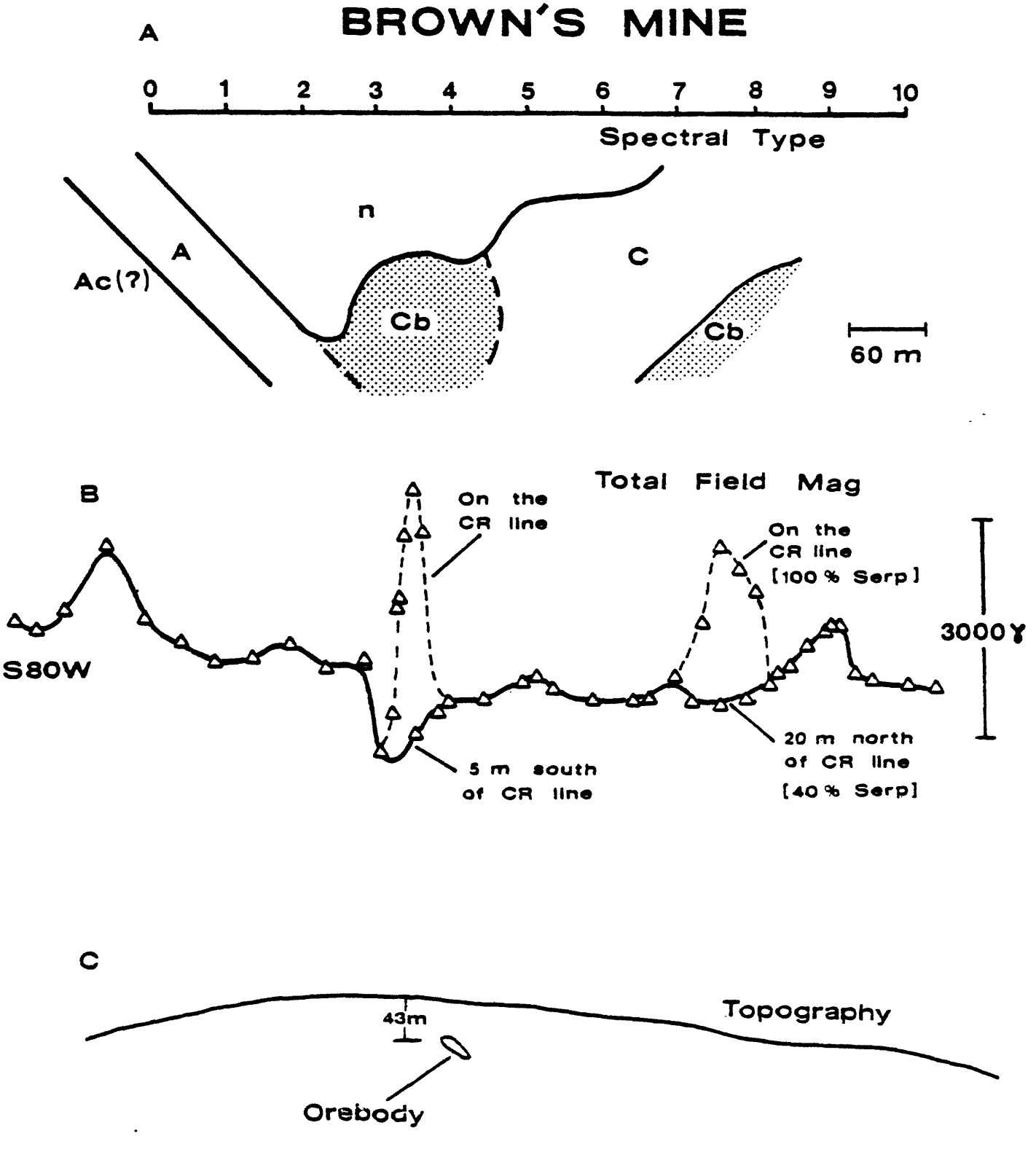
A
BROWN'S MINE
0 1 2 3 4 5 6 7 8 9 10
Spectral Type
n
A
Ac(?)
Cb
C
Cb
60 m
B
Total Field Mag
On the CR line
On the CR line [100 % Serp]
3000γ
S80W
5 m south of CR line
20 m north of CR line [40 % Serp]
C
43m
Topography
Orebody

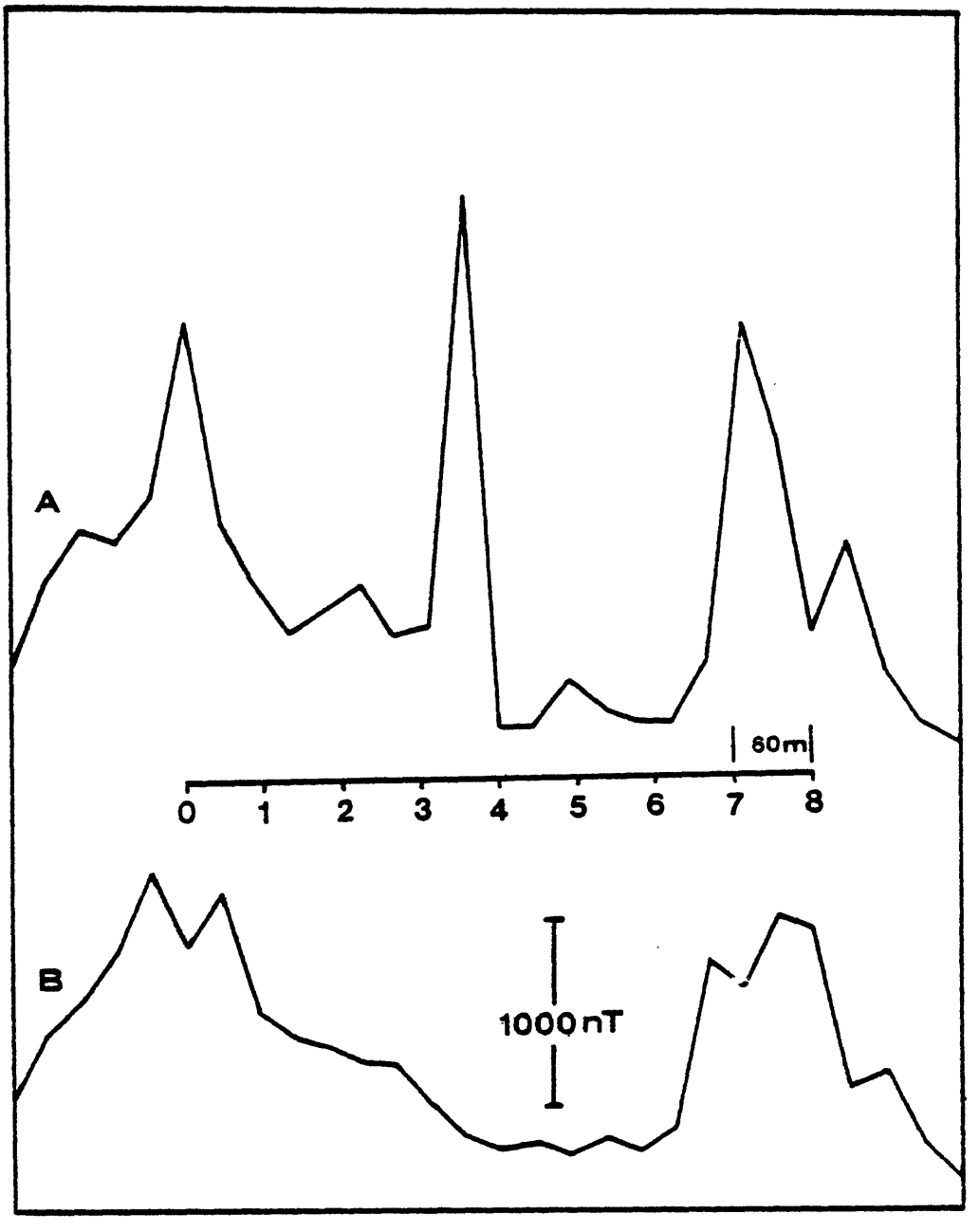
A
60m
0 1 2 3 4 5 6 7 8
B
1000nT